Supplement to Cechova, Vegesna, et al.

www.pnas.org/cgi/doi/10.1073/pnas.2001749117

Supplemental Methods

Short- and long-read data to generate Y chromosome assemblies

We used human and chimpanzee Y sequences from version hg38 and panTro6 assemblies, respectively (1, 2). In both cases, PARs were masked (we used human coordinates 10,001-2,781,479 and 56,887,903-57,217,415 for PAR1 and PAR2, respectively, as provided by ENSEMBL (https://useast.ensembl.org/info/genome/genebuild/human_PARS.html) and 26,215,992-26,350,515 for PAR in chimpanzee, identified in house using LASTZ (3) alignments). For the gorilla Y chromosome, there are two published assemblies: the one produced from short- and long-read data by our group (4), and the one recently generated using PacBio reads pre-processed with PACASUS to remove within-read duplications (5). We merged the two assemblies to obtain a more continuous and complete version; the merging was performed with METASSEMBLER v.1.5 (6). Since METASSEMBLER additionally uses information from mate-pair reads, we used the previously-generated GY19 library (4) and set insert sizes to range from 298 to 6,444 bp in the configuration file.

For both orangutan and bonobo (**Fig. S1**), we first generated short, paired-end reads for a male individual. Sumatran orangutan male (ID 1991-51) genomic DNA provided by the Smithsonian Institution was extracted from testis using DNeasy Blood and Tissue Kit (Qiagen). Bonobo male (ID PR00251) genomic DNA was extracted using the same kit from the fibroblast cell line provided by the San Diego Zoological Society. Illumina paired-end PCR-free libraries with insert size of ~1,000 bp were constructed from both DNA samples and sequenced on HiSeq2500 using 251-bp paired-end sequencing protocol (approximately 600 million reads were generated for each library). The reads were assembled using DISCOVAR (7). To identify putative Y-chromosomal contigs, we processed each of these two male assemblies with DISCOVERY (8) using the male-to-female abundance threshold of 0.4 and using "-abundance-min 4". The resulting contigs were scaffolded with filtered mate-pair 250-bp reads, generated for the same individuals using Nextera Mate Pair Sample Preparation Kit (with median insert size of 8 kb), using BESST v.2.2.8 (9). Filtering of mate pairs was performed as follows. All mate-pair reads were mapped to the respective (bonobo or orangutan) whole-genome male DISCOVAR assembly using BWA-MEM v.0.7.17-r1188 (10). From these alignments, reads putatively originating from Y chromosome were retained and used for scaffolding. The next step, aimed at further improving the continuity of Y assemblies, differed between orangutan and bonobo. The orangutan Y assembly was merged (using METASSEMBLER v.1.5 (6)) with an assembly generated for orangutan male AG06213 with 10×Genomics (**Table S10**). To aid METASSEMBLER, one can provide mate-pair reads; we used mate-pair reads from individual 1991-51 and set the insert size range from 5,088 to 12,683 bp in the configuration file. High-molecular-weight genomic DNA from Sumatran orangutan male (ID AG06213) was extracted from fibroblast cell line (provided by L. Carrel, PSU) using MagAttract HMW DNA kit (Qiagen) and used to construct a 10x Genomics library. The resulting reads were assembled with SUPERNOVA assembler v.1.0.2 (11). The bonobo Y assembly was augmented with PACASUS-corrected (default parameters) (5) flow-sorted Y-enriched PacBio reads from a bonobo male Ppa_MFS using SSPACE-LONGREAD (v.1-1) (12), and additional scaffolding and assembly were performed with PBJELLY (PBSuite_14.9.9, parameters <blasr>-minMatch 8 -minPctIdentity 85 -bestn 1 -nCandidates 20 -maxScore -500 -nproc 6 -noSplitSubreads</blasr>) (13).

The subsequent processing steps were the same for the orangutan Y and bonobo Y assemblies. For the orangutan, we first called variants from the first male (ID 1991-0051) relative to the assembly we obtained after merging with 10×Genomics data. The variants were called with FREEBAYES (v.1.3.1) (14) using settings "--ploidy 1 --min-alternate-fraction 0.6", and filtered for quality (biopet-vcffilter --minQualScore 30). We then used BCFTOOLS to 'polish' the assembly by consensus calling (BCFTOOLS consensus -H 1, **Table S11**). Using the same approach, we polished the bonobo Y assembly using the variants from bonobo male ID PR00251.

To remove the pseudoautosomal region (PAR) and potential residual autosomal contamination, all scaffolds in gorilla, bonobo and orangutan Y assemblies were filtered against corresponding gorilla (gorGor4), bonobo (panPan2), and orangutan (ponAbe3) female reference genomes. We mapped the assembly scaffolds to the female reference using BLASR v.5.3.3 (15) with parameters: "blasr --bestn 1 --nproc 32 --hitPolicy randombest --header --minPctSimilarity 95". Scaffolds that had at least 95% sequence identity to the female genome were excluded from the assemblies. Female reference genomes were based on hg38, panTro6, gorGor4, ponAbe3, and panPan2 assemblies for human, chimpanzee, gorilla, orangutan, and bonobo, respectively.

Multi-species alignments

To align the Y chromosomes of five great ape species, several alignment algorithms were evaluated: SIBELIAZ (16), MULTIZ-TBA (17), MULTIZ-ROAST (17), and PROGRESSIVECACTUS (18). The alignments were evaluated both by comparing the proportion of aligned base pairs and visually, i.e. by comparing the assembled coverage in non-human great ape species sequences aligned to the human X-degenerate genes. PROGRESSIVECACTUS showed the most promise and was chosen for all further analyses. We soft-masked repeats prior to the alignment of assemblies using REPEATMASKER (19) with the following settings: *RepeatMasker -pa 63 -xsmall -species Primates ${assembly}.rmsk.fa* (19). To generate multiple sequence alignment with PROGRESSIVECACTUS, we used default parameters and did not provide a guide tree. The alignment was converted from hal (20) to MAF format using HAL2MAF (parameterized with, for example, --noAncestors --refGenome hg_Y --maxRefGap 100 --maxBlockLen 10000). The role of the MAF reference sequence was given to each species in turn, to create a separate MAF file for each, as well as for the PROGRESSIVECACTUS-inferred ancestral sequence.

We split the MAF file by species subset, producing a separate MAF file containing all blocks that only involve the particular species in that subset. The MAF file of blocks containing all five species was converted to MULTI-FASTA by MAF to FASTA tool, run at https://usegalaxy.org/ (GALAXY version 1.0.1), using an option "One Sequence per Species". Sequence identity was calculated from the MULTI-FASTA file using the custom script multi_fasta_to_pairwise_identity.py.

Independently, sequence identity distributions were derived from pairwise alignments as follows. For each pair of species (s1, s2) LASTZ (3) was used to align s1's Y assembly and s2's. Masking was disabled, allowing alignment of duplicated elements. Substitution scores were identical to those used by us in Tomaszkiewicz et al. (4). The exact LASTZ command line was: "lastz s1.chrY[unmask] s2.chrY[unmask] W=12 Q=human_primate.scores." Alignments were then post-processed as follows. For each base in s1, the highest identity alignment covering that base was chosen, and base counts were collected for identities at 0.1% intervals. Average sequence identity was computed from these binned counts, excluding any unaligned bases.

Percentage of sequence aligned in multiple alignment was computed as follows. For the portion of species s1 aligning to s2, all MAF blocks containing s1 and s2 (as well as, possibly, other species) were extracted. These were reduced to the aligning intervals in s1 by computing the mathematical union of all s1 intervals in any of the extracted blocks. The combined length of these intervals is the number of bases in s1 that have an alignment to s2. This length was divided by the number of non-N bases in s1.

Percentage of sequence aligned in pairwise alignments was computed as follows. For the portion of species s1 aligning to s2, the s1-to-s2 LASTZ alignment was reduced to the aligning intervals in s1 by computing the mathematical union of all s1-intervals in any alignment block. The combined length of these intervals is the number of aligning bases in s1. This length was divided by the number of non-N bases in s1.

Substitution rate analysis

To estimate the substitution rates on the Y chromosome, we used the ancestor-based five-species alignment described in the previous section. To provide conservative estimates of substitution rates, we removed duplicates from the alignment using MAFDUPLICATEFILTER from the MAFTOOLS suite (version 0.1) (21), similar to (22). This step replaces multiple sequences from the same species by the sequence closest to the consensus of an alignment block. We also converted all alignments blocks to the positive strand of the ancestral sequence (maf_flip_for_ref.py). Again, to obtain conservative estimates, we only retained alignment blocks where all five species were present, thus largely restricting our analysis to X-degenerate regions. This step was performed using script *parse_cactus* (available on GITHUB) and the python libraries *bx.align.maf* and *bx.align.tools*. The final filtered alignment was then used to pick the best-fitted substitution model using JMODELTEST (23, 24). Taking into account AIC and BIC of the various models tested with JMODELTEST and the availability of models implemented in PHYLOFIT (25), we decided to proceed with GTR (also called REV) model (26) with variable substitution rates (--nrates=4). Using this model and our filtered alignment, we ran PHYLOFIT (25) with the following settings: phyloFit -E --subst-mod REV --nrates 4 --tree "(((hg_Y,(panTro_Y,panPan_Y)),gorGor_Y),ponAbe_Y)". The estimated branch lengths were used for all the downstream analysis. The output was then visualized using R script and library APE (27)(28).

Gene content analysis

Analysis of genes homologous to human Y genes. To retrieve the bonobo and orangutan Y chromosome X-degenerate and ampliconic genes, we aligned the scaffolds from bonobo and Sumatran orangutan Y chromosome assemblies to species-specific or closest-species-specific reference coding sequences using BWA-MEM (v.0.7.10) (10). Next, we visualized the alignment results in Integrative Genomics Viewer (IGV) (v.2.3.72), and protein-coding consensus sequences were retrieved and checked for ORFs. However information about *RPS4Y2* and *MXRA5Y* remained missing. We used gene predictions (see next paragraph) and testis-specific transcriptome assemblies (29) from the same publication to study the presence of the *RPS4Y2* and *MXRA5Y* genes (**Fig. S6**).

Predicting novel genes in bonobo and orangutan assemblies. We used AUGUSTUS (30) (--species=human --softmasking=on --codingseq=on) to predict genes in the Y chromosome assemblies of bonobo and orangutan. From the list of predicted genes we retained those that have a start and stop codon. Using BLASTP from BLAST (2.9.0; -db uniprot_sprot.pep -max_target_seqs 1 -evalue 1e-5 -num_threads 10) (31) we annotated the predicted gene sequences. Based on BLAST annotation, we classified all the genes which are not annotated by BLASTP as candidate *de novo* genes. From these genes, we retained those that had >90% sequence identity to the sequence in the UniProt (32) protein database and were covered by at least 90% of the gene sequence in the BLAST output. To make sure that the predicted genes are on the Y chromosome and do not represent misassemblies, we performed an extra filtering step where we used only those genes which are present on contigs which align to either human or chimpanzee Y chromosomes. The resulting gene annotations which are not found on the human Y chromosome were assigned as candidate novel genes translocated to the Y. The longest predicted transcript sequences for genes annotated as Y-chromosome-specific were obtained without the above filters for validation of missing gene content in bonobo and orangutan. The gene predictions which were annotated as X homologs (*TXLNG*, *PRKX*, *NLGNX*, etc.) of Y chromosome genes were also classified as Y genes.

Reconstruction of gene content evolution in great apes. Once we obtained the complete Y chromosome gene content in great apes, we converted the gene content into binary values which represent the presence or absence of a gene in a species. The complete deletion or pseudogenization of gene/gene families is represented by ‘zero’ and the presence of an uninterrupted gene is represented by ‘one’. Using the model developed by Iwasaki and Takagi (33), we reconstructed the evolutionary history of (separately ampliconic and X-degenerate) genes across great apes. The phylogenetic tree of great apes (34), along with the table representing the presence or absence of genes (**Fig. S6**), was used as an input to generate the rate of gene

birth and gene death for each branch of the tree, and the reconstructed gene content at each internal node of the tree. To obtain the rate in the units of events per million years, the rate of gene birth, as well as the rate of gene death, was divided by the length of the branches (in millions years) (33).

Palindrome analysis

Human and chimpanzee palindrome arm sequence conservation. The PROGRESSIVECACTUS output file was converted to MAF (see the preceding paragraph) twice. The first time we set --refGenome to 'human', which results in a human-centric MAF file (where the first line represents sequences from the human Y) and the second time we set --refGenome parameter to 'chimpanzee' to obtain a chimpanzee-based MAF file. The coordinates of the human and chimpanzee palindromes (PanTro4) were obtained from a previous publication (4). Chimpanzee palindrome coordinates were converted to the PanTro6 version using the LIFTOVER utility from the UCSC Genome Browser (35). For few chimpanzee palindromes for which LIFTOVER failed to convert the coordinates, we generated a dotplot of chimpanzee Y to itself using GEPARD (36) and identified the locations of palindromes from the dotplot. To overcome redundancy of sequence between the arms of palindrome, we further obtained the coordinates of the first arm of the palindrome for human (**Table S12A**) and chimpanzee (**Table S12B**), from which the palindrome coverage was calculated.

With the use of ALIGNIO from BIOPYTHON (37), we parsed the MAF files to obtain all the alignment blocks which overlapped given palindrome arm coordinates for each species and summed the number of sites covered by these parsed alignment blocks. For each alignment block within the palindrome arm, we considered only those sequences which had less than 5% gaps and counted the number of aligned nucleotides per species at sites where the palindrome arm is unmasked (softmasked with REPEATMASKER (19)). Next we calculated the number of nonrepetitive characters in the whole palindrome arm and used it to calculate the percentage of non-repetitive alignment within the palindrome arm per species.

Palindrome sequence read depth in bonobo, gorilla, and orangutan. We used a pre-established pipeline used to identify human and chimpanzee palindrome sequences in Y assemblies (4). The bonobo, gorilla, and orangutan Y contigs were broken into non-overlapping 1-kb windows and each window was aligned to human (hg38) and (separately) chimpanzee (panTro6) Y chromosome sequences using LASTZ (version 1.04.00) (--scores=human_primate.q, --seed=match12, --markend) (3) separately. The substitution scores were set identical to those used for published LASTZ alignments of primates (38). The best alignment for each window was retrieved from the LASTZ output. All the windows with alignments of >800 bp were considered as homologs to human or chimpanzee Y palindromes and used in the downstream analysis.

The whole-genome male sequencing reads from orangutan, gorilla, and bonobo (**Table S10**) were mapped to the human and (separately) chimpanzee Ys using BWA-MEM (version 0.7.17-r1188)(10) and the resulting output files were sorted and indexed using samtools (version 1.9) (39). Using COMPUTEGCBIAS and CORRECTGCBIAS functions from DEEPTOOLS (version 3.3.0) (40), we performed GC correction of the sequencing read depths. Finally, using BEDTOOLS (v2.27.1)(41) 'coverage' function, we obtained the read depth of the windows homologous to human and chimpanzee palindrome sequences (of whole palindromes) identified as described in the previous paragraph. We compared the read depths of palindromic sequence windows to that of windows overlapping X-degenerate genes.

Finding the copy number for ampliconic regions that are species-specific. From the multiple sequence alignment of the Y chromosomes of great apes (species-centric), we extracted the alignment blocks which were unique to a particular species and not aligned to the other Y chromosomes. We filtered the species-specific blocks which were >100 bp in size and obtained their GC-corrected read depth from male whole-genome sequencing data (we used data from paired-end sequencing libraries in **Table S10**). To calculate the copy number of the resulting blocks we divided their read depth by the median read depth of

windows which overlap X-degenerate genes from the palindrome copy number analysis (read depth of single-copy regions).

Search for regulatory factor binding sites in human palindromes P6 and P7. We checked for the presence of sites specific to DNA binding proteins on human palindromes P6 and P7, which could imply the presence of functionality related to gene regulation. Initially we used the ENCODE track (http://genome.ucsc.edu/ENCODE/) at the UCSC Genome Browser (35) to search for epigenetic modifications in the palindrome regions (42). In particular, we used the track from the Bernstein Lab at the Broad Institute containing H3K27Ac and H3K4Me1 data on seven cell lines from ENCODE, from which we identified human umbilical vein endothelial cells (HUVEC) to have signals in palindrome P6. Later we extended our search to ENCODE data portal (https://www.encodeproject.org/) from where we downloaded the BAM files to look for the presence of peaks (**Table S13**)(43). We used the "Search by region" page under Data in the ENCODE data portal (https://www.encodeproject.org/region-search/) and GRCh38 setting to search for files which are related to the coordinates of palindromes P6 (chrY:16159590-16425757) and P7 (chrY:15874906-15904894). The resulting files were visualized in the UCSC Genome Browser to identify signals in the peaks, and from this information we identified signals in human liver cancer cell line HepG2 for P7. The current ENCODE data processing pipeline by default filters out reads with low mapping quality (i.e. mapping in multiple places of the genome), as a result we did not find any peaks/signals in the majority of the datasets (https://www.encodeproject.org/pipelines/). To overcome this limitation, we manually downloaded the unfiltered BAM files (HUVEC: H3K27Ac, H3K4Me1 and DNase-seq; Testis:H3K27Ac, H3K4Me1 and Dnase-seq; and HepG2: CREB1; Table S13), which include low-mapping-quality reads. We performed peak calling using MACS2 (version2.1.4; -f BAM --broad --broad-cutoff 0.05) (44) and the control samples were used whenever available. We used integrative genomics viewer (IGV) (version 2.4.19)(45) to visualize the data.

Hi-C analysis. We used MHI-C (46) to process the Hi-C data generated by (47). Both human and chimpanzee samples originated from pluripotent stem cells (iPSCs), processed with protocol using *Mbo I* restriction enzyme (with the GATCGATC recognition site) and sequenced on Illumina Hi-Seq 4000. The sequencing reads were downloaded from SRA (accessions SRR1658709 and SRR8187262 for human and chimpanzee, respectively) and subsampled to the first 100 million reads. The original MHI-C scripts were modified to match the reference genome and other settings; the resolution was set to 10,000, cutsite was set to 0, and normalization method was set to KR (48) with uniPrior (built based on unique bin pairs within valid interaction distance, see https://github.com/keleslab/mHiC). Additionally, we analyzed a biological sample extracted from umbilical vein endothelial cells of a newborn male, cultured in cell line HUVEC (CC-2517), further subjected to the *in situ* Hi-C protocol with *Mbo I* restriction enzyme and sequenced on Illumina HiSeq 2000 (49). For this analysis, we used the first 50 million reads of SRR1658570 dataset.

In order to calculate the enrichment of ampliconic interactions, we defined these regions separately in human and chimpanzee. In human, we used the corresponding coordinates of eight palindromes (4). Because chimpanzee Y is composed of a higher number of intertwined amplicons and 19 palindromes, the continous ampliconic part spanning the *q* arm of this chromosome, as well as a large part of *p* arm adjacent to the centromere, was analyzed as a single unit.

Supplemental Notes

Supplemental Note S1. Developing a classifier and evaluating it.

We developed a classifier to determine which assembly scaffolds are ampliconic and which are X-degenerate. Ideally, Y ampliconic regions would have a higher copy number in the reference genome than X-degenerate regions, however, Y ampliconic regions are often collapsed in next-generation-sequencing-based assemblies (50). Our classifier therefore combines the copy count in the reference with mapping read depth information, since collapsed Y ampliconic regions will have a higher number of mapping reads than single-copy X-degenerate regions, in whole-genome-sequencing datasets originating from male individuals (using paired-end sequencing reads from respective species described in **Table S10**). We proceeded to classify scaffolds in our orangutan, bonobo, and gorilla Y assemblies (such annotations are already available in the human and chimpanzee Y assemblies (1, 2)). We examined scaffolds carrying coding sequences of known X-degenerate and ampliconic genes (Table SN1A). The classification was successful in the vast majority of cases (accuracy was 85%, 100%, and 88% for bonobo, gorilla, and orangutan, respectively, Table SN1A).

Table SN1A. The number of X-degenerate and ampliconic genes that were confidently mapped to scaffolds classified as X-degenerate or ampliconic, per our classifier.

Species	Gene type	Classified as X-degenerate	Classified as ampliconic
GORILLA	ampliconic	2	**5**
	X-degenerate	**12**	1
BONOBO	ampliconic	1*	**5**
	X-degenerate	**9**	0
ORANGUTAN	ampliconic	1	**2**
	X-degenerate	**5**	0

**BPY* is present in a single copy in gorilla

Additionally, to validate our classification method, we ran our pipeline (see Methods) on human and chimpanzee Y chromosomes (excluding pseudoautosomal regions), by simulating human and chimpanzee reads. Y reads were simulated from the Y reference using wgsim (https://github.com/lh3/wgsim) and parameters -S 9 -1 101 -2 101. Next, to make the reference human and chimpanzee Y assemblies more similar to the next-generation sequencing assemblies we generated for bonobo, gorilla, and orangutan, we used panTro6 and hg38 Y chromosome references and masked one arm of each palindrome in order to mimic the collapse of highly similar ampliconic regions. These masked references for human and chimpanzee Y chromosomes were split into consecutive 150-kb and 100-kb scaffolds, respectively, reflecting shorter palindrome arms in chimpanzee than in human. These sizes are similar to N50/NG50 statistics for our newly generated assemblies (Table S1). We filtered out scaffolds that contained more than 20% of Ns using sequence_cleaner (https://biopython.org/wiki/Sequence_Cleaner) and parameters 0 20. For the remaining scaffolds, we ran our pipeline using the reads simulated as described above. We examined the classification of scaffolds carrying coding sequences of known X-degenerate and ampliconic genes (Table SN1B; Fig. S4).

Table SN1B. The number of X-degenerate and ampliconic genes that were confidently mapped to scaffolds classified as X-degenerate or ampliconic, per our classifier.

Species	Gene type	Classified as X-degenerate	Classified as ampliconic
HUMAN	ampliconic	4	**7**
	X-degenerate	**12**	2

CHIMPANZEE	ampliconic	5	**15**
	X-degenerate	**13**	1

The accuracy of classification was 76% for human and 82% for chimpanzee, which is satisfactory, but somewhat lower than that for our bonobo, gorilla, and orangutan assemblies, perhaps because our simulated human and chimpanzee scaffolds were not entirely reflective of the copy-number distribution in the next-generation sequencing assemblies. In line with this reasoning, we found three scaffolds in human (two for *TSPY* and one for *RBMY*) and two in chimpanzee (*RBMY* and *TSPY*) erroneously classified as X-degenerate, presumably because these genes are located in repetitive parts of the Y chromosome that were not masked with our method; in human *TSPY* is located in a tandem array outside of palindromes (which we did not mask), whereas *RMBY* is located in inverted repeat 2 (which we did not mask) and in palindrome P3 (which we masked).

Methods

To classify scaffolds as either ampliconic or X-degenerate (PAR regions have been filtered out in our assemblies), each assembly was divided into 5-kb windows with 2-kb overlaps. First, for each window, we calculated copy number using a modified version of AMPLICONE (51) that can handle scaffolds instead of a single continuous reference. AMPLICONE takes into account mappability (calculated using the GEM mappability program (52) for k=101), repetitive element content as provided by REPEATMASKER (Open-4.0.7, RepBaseRepeatMaskerEdition-20181026), and performs GC correction. X-degenerate regions are expected to have similar copy number estimates (i.e. estimates based on sequencing depth), whereas copy number estimates for ampliconic regions are expected to be higher and vary greatly, depending on the copy number of the underlying amplicons in the genome and in the assembly. Fully resolved amplicons, such as palindrome arms, are present multiple times in the assembly, and thus each window carrying them maps equally well to multiple places in the assembly. Thus, all windows were mapped back to the assembly and, after excluding secondary alignments, all multi-mapping windows were flagged as potentially ampliconic (windows with MAPQ=0 as produced by BWA-MEM (10)). If a window was both nonrepetitive (non-zero copy number by AMPLICONE) and multi-mapping, it was assigned as ampliconic. Additionally, all uniquely mapping windows (MAPQ=60) with high copy number for species-specific thresholds (see Table SN1C) were also assigned as ampliconic. Uniquely mapping windows (MAPQ=60) with copy number below the species-specific thresholds were assigned as X-degenerate. This led to the majority of windows classified as either ampliconic or X-degenerate. Two types of windows remained unassigned; those that map uniquely but contain no copy-number information from AMPLICONE, and those that contain copy-number information but have mapping quality below 60. All such windows had their assignment interpolated. As these windows were internally represented as missing values (NA), we used na.approx function from the R package zoo (53). Each scaffold was then classified as either ampliconic or X-degenerate based on the majority vote of all underlying windows. A small subset of our assemblies (0.12, 0.33, and 0.71 Mb in bonobo, gorilla and orangutan) remained unclassified.

Table SN1C. The copy-number thresholds for X-degenerate (<) and ampliconic (≥) windows, the size of the classified ampliconic and X-degenerate regions, and the corresponding number of scaffolds.

	Gene type	threshold	size [Mb]	# scaffolds
GORILLA	ampliconic	0.95	3.95	71
	X-degenerate		10.02	161
BONOBO	ampliconic	0.5	10.8	2,521
	X-degenerate		12.5	967
ORANGUTAN	ampliconic	0.75	2.2	670

	X-degenerate		14.5	358

For validation, we mapped coding sequences of X-degenerate and ampliconic genes from chimpanzee, gorilla, and Sumatran orangutan to verify that the scaffolds carrying these genes were classified correctly. We required strict mapping to avoid false hits; first we used blat (v. 36) with default parameters and then required at least thirty matches (matches≥30), the recovery of at least 20% of the original coding sequence query ((matches/qSize)≥0.2), and 99% of matching bases ((matches/(matches+misMatches))≥0.99). All accompanying scripts are available from https://github.com/makovalab-psu/great-ape-Y-evolution and in-house scripts *run_copy_number.sh* and evaluate.sh that output the annotation of scaffolds as a .gff file.

Supplemental Note S2. Male mutation bias.

Using branch-specific values for autosomal and Y-chromosomal substitution rates from Fig. 1, we obtained the following values of α, or the male-to-female substitution rate ratio (54):

Species	Substitution rate on the Y	Substitution rate on autosomes (A)	Y/A	α
Human	0.0096	0.0066	1.45	2.678
Chimp	0.0037	0.0021	1.76	7.40
Bonobo	0.0041	0.0025	1.64	4.56
Gorilla	0.0150	0.0089	1.69	5.36
Orang	0.0564	0.0268	2.10	∞
BC	0.0082	0.0046	1.78	8.20
BCH	0.0045	0.002	2.25	∞

The species-specific estimates of α we obtained above follow the trend observed in our previous study (see Table 1 in (55)) based on a comparison of substitution rates at a much shorter genetic region (~10 kb) homologous between chromosomes Y and 3. Namely, we also observe that α is lower in human than in bonobo or gorilla. Note that our estimates are derived from closely related species and thus might be inaccurate because of ancient genetic polymorphism (55). This phenomenon is difficult to correct for in branch-specific estimates. However, it can be accounted for in pairwise estimates.

Focusing on pairwise comparisons we presented in the Results, we computed α using both uncorrected and corrected by ancestral polymorphism autosomal rate estimates. In primates, the Y chromosome has much lower diversity than autosomes do (56), and thus we did not correct for it. The results are shown below:

	Y	A	Y/A	α	Corrected A*	Corrected Y/A	Corrected α
Gorilla-human	0.0291	0.0175	1.66	4.93	0.01592	1.83	10.62
Gorilla-chimp	0.0314	0.0176	1.78	8.26	0.01602	1.96	49.06
Gorilla-bonobo	0.0319	0.0180	1.77	7.78	0.01642	1.94	33.94

*We subtracted 0.00158 -- the diversity estimated from gorilla populations (57) -- from our autosomal substitution rate estimates.

Again, consistent with the data presented in Results, we observed larger differences between the Y chromosomal and autosomal substitution rate estimates for gorilla-chimpanzee and gorilla-bonobo comparisons, than for the gorilla-human comparisons.

We also evaluated the potential effect of ancient genetic polymorphism on the ratio of pairwise estimates of autosomal substitution rates we present in Results. We found that this effect is minimal.

	Y	A uncorrected	A ratio	A corrected*	Corrected ratio to gorilla-human comparison
Gorilla-human	0.0291	0.0175		0.0159	
Gorilla-chimp	0.0314	0.0176	1.006	0.0160	1.0063
Gorilla-bonobo	0.0319	0.018	1.029	0.0164	1.0314

*We subtracted 0.00158 - the diversity estimated from gorilla populations (57) -- from the autosomal substitution rate.

Supplemental Note S3. AUGUSTUS gene predictions.

AUGUSTUS (30) predicted 219 genes on the bonobo Y assembly, of which 25 complete or partial genes represent homologs of known human protein-coding genes. In the case of Sumatran orangutan, AUGUSTUS predicted 90 genes of which 33 complete or partial genes represent homologs of known human protein-coding genes. After implementing requirements of gene predictions (1) to have start and stop codons, and (2) be present on contigs that align to human or chimpanzee Y, we did not find any novel genes on the Y chromosome of orangutan, however we found two candidates—*SUZ12* and *PSMA6*—which have >95% identity and >90% coverage to the gene homologs on the autosomes of bonobo.

A possible transposition of the autosomal *SUZ12* gene (located on human chromosome 17) onto the bonobo Y chromosome was predicted (Table SN3) based on the limited number of introns (one intron), in contrast to its autosomal homolog, which has 15 introns (NM_015355). The *SUZ12* gene has no matches to human and gorilla Y, however the first 121 bp of its predicted sequence align to chimpanzee (palindromes C2, C11 and C15) and orangutan Y. However, when we aligned testis RNA-seq data to the predicted *SUZ12* gene on the bonobo Y chromosome, the first exon with the start codon was not expressed (Fig. SN3A), whereas the second exon was expressed (Fig. SN3B). The single nucleotide variants in the RNA-seq reads mapping to the second exon are consistent with the variants of the *SUZ12* gene present on chromosome 17. Thus, we concluded that the translocated *SUZ12* was pseudogenized on bonobo Y.

The *PSMA6* gene was also predicted in bonobo, which shared 99.6% identity with its homolog on the chimpanzee Y and 97.8% identity on human Y. However, there were no homologous sequences in the orangutan and gorilla Y assemblies. The *PSMA6* gene on human Y was annotated as a pseudogene in the Entrez database (Gene ID: 5687). Therefore, we concluded that *PSMA6* is also a pseudogene on the bonobo. Thus, no novel genes, as compared to the human Y chromosome genes, were found on the bonobo and orangutan Y chromosomes.

Table SN3. Gene annotation of the *SUZ12* homolog on the bonobo Y, as predicted by AUGUSTUS

Sequence name	Feature	Start	End	Strand
Contig591	gene	74	61572	-
Contig591	transcript	74	61572	-
Contig591	stop_codon	74	76	-
Contig591	CDS	74	2353	-
Contig591	CDS	61453	61572	-
Contig591	start_codon	61570	61572	-

Figure SN3A. The IGV (45) **view of the first exon of the SUZ12 homolog on the bonobo Y.** Testis-specific RNA-seq reads (SRA ID: SRR306837) were mapped to bonobo Y assembly using BWA-MEM (10).

Figure SN3B. IGV view of second exon on SUZ12 homolog on bonobo Y. Testis specific RNASeq reads (SRA ID: SRR306837) were mapped to bonobo Y assembly using BWA-MEM (10).

Supplemental Note S4. Analysis of X-Y gene conversion and selection.

Gene conversion. Prior to analyzing selection, we had to perform an analysis of X-Y gene conversion, as this process can interfere with selection detection. We studied the incidence of X-Y gene conversion between 12 X-degenerate genes and their homologs on the X chromosome (from 16 X-degenerate genes present on the human Y we excluded *CYorf15A*, *CYorf15B*, *RPS4Y1*, and *RPS4Y2,* as parts of these genes have repeats on the Y and homologs on the X, making detection of gene conversion difficult). Gene conversion was examined using a multiple-sequence alignment of the X and Y chromosomes.

We softmasked the X and Y chromosomes of great apes using REPEATMASKER (19) (RepeatMasker -pa 63 -xsmall -species Primates ${assembly}.rmsk.fa). PROGRESSIVECACTUS (18) was used to align the chromosomes. A guide tree which pairs the X and Y chromosomes from the same species list was used (((chimpY, chimpX),(bonoboY, bonoboX),(humanY, humanX),(gorillaY, gorillaX),(sorangY, sorangX))). The resulting alignment output from PROGRESSIVECACTUS was converted to MAF format by HAL2MAF (20) using human Y as a reference (--noAncestors --refGenome humanY --maxRefGap 100 --maxBlockLen 10000). We then parsed the alignment blocks (retaining blocks longer than >50bp; range of gene conversion tracts we observed in human was 55-290 bp, as was observed in previous studies (58, 59)) which fall within the coordinates of X-degenerate genes. We did not perform additional filtering based on repeat content within the alignment blocks. For each block, the alignments which constitute the sequences from both the X and Y chromosomes for a species were collected in a FASTA file. We used GENCONV (60) (/w9 /lp -nolog) to identify gene conversion events based on multiple sequence alignment files. By default, the output of GENCONV constitutes a global list of high-confidence gene conversion events after multiple testing for each sequence pair. We also used /lp parameters with which a second list of significant gene conversions for all possible pairwise comparisons GENCONV performed was generated. We used a p-value cutoff of 0.05, as GENCONV provides p-values after correcting for multiple comparisons. We used pairwise comparisons to address gene conversion in cases where a chromosome was represented by more than one sequence in the alignment. From the GENCONV output, we parsed events that constitute gene conversion between the X and Y chromosome from the same species and retained events which are longer than 50 bp.

In total, we detected 143 candidate gene conversion events up to 50-410 bp in length (minimal length of 50 bp was used for detection), including 46 high-confidence ones (Table SN4A; Table SN4B). Among these, most events were observed in the genes from younger strata—30 in *PRKY* (stratum 5), nine in *NLGN4Y* (stratum 4), four in *AMELY* (stratum 4), and two in *TBL1Y* (stratum 4). Higher homology between these genes and their X homologs, as opposed to between genes from older strata and their X homologs, is expected to facilitate gene conversion, which work most efficiently with homology >92% (58). No gene conversion events >50 bp in size were found in the exonic regions of X-degenerate genes, thus this process should not affect our selection analysis.

Table SN4A. Gene conversion between X and Y chromosomes of great apes using GENECONV. The values represent the number of high-confidence gene conversion events with significant *p*-values (<0.05) which are corrected for multiple comparisons across all sequence pairs. The values in brackets represent the total number of gene conversion events with significant *p*-values (<0.05) for comparisons corrected for the length of the alignment.

Gene (Stratum)	Bonobo	Chimpanzee	Human	Gorilla	Orangutan	Total
***AMELY* (4)**	1 (1)	1 (1)	1 (1)	1 (1)	0	4 (4)
***DBY* (3)**	0 (1)	0 (1)	0	0	0 (1)	0 (3)
***EIF1AY* (3)**	0	0	0	0	0	0
***KDM5D* (2)**	0	0	0	0	0	0
***NLGN4Y* (4)**	2 (6)	2 (7)	3 (7)	1 (8)	1 (3)	9 (31)

***PRKY* (5)**	8 (25)	10 (27)	4 (17)	8 (17)	0	30 (86)
***SRY* (1)**	0	0	0	0	0	0
***TBL1Y* (4)**	1 (4)	0 (2)	1 (7)	0 (3)	0 (2)	2 (18)
***TMSB4Y* (3)**	0	0	0	0	0	0
***USP9Y* (3)**	0	0	0	0	0	0
***UTY* (3)**	0	0	0	0	0	0
***ZFY* (3)**	0	0	0	0	1 (1)	1(1)
Total	12 (37)	13 (38)	9 (32)	10 (29)	2 (7)	46(143)

Table SN4B. Human-specific coordinates of high-confidence X-Y gene conversion events in great apes. Second column indicates the human-specific coordinates within multiple sequence alignment (MSA) of great ape X-Y chromosomes generated using PROGRESSIVECACTUS (18). Third column indicates the species in which X-Y gene conversion was observed. The last two columns indicate the start and end positions within the alignment where gene conversion was observed.

Gene	**Human-specific coordinates**	**Species**	**P-value**	**Start**	**End**
AMELY	chrY:6866332-6866529	gorilla	0.0477	42	91
AMELY	chrY:6866332-6866529	human	0.0071	42	112
AMELY	chrY:6866332-6866529	bonobo	0.0143	42	133
AMELY	chrY:6866332-6866529	chimpanzee	0.0318	42	133
NLGN4Y	chrY:14529557-14529930	chimpanzee	0.0002	251	335
NLGN4Y	chrY:14603265-14603446	orangutan	0.0083	75	125
NLGN4Y	chrY:14676028-14676264	human	0.0153	42	119
NLGN4Y	chrY:14681897-14682244	bonobo	0	1	199
NLGN4Y	chrY:14687977-14688352	gorilla	0.044	40	112
NLGN4Y	chrY:14717874-14718034	human	0.0204	79	134
NLGN4Y	chrY:14727969-14728395	bonobo	0.0136	133	250
NLGN4Y	chrY:14727969-14728395	chimpanzee	0.0116	133	250
NLGN4Y	chrY:14759856-14760011	human	0.0144	57	108
PRKY	chrY:7285434-7285938	chimpanzee	0.0023	1	167

PRKY	chrY:7286596-7286731	gorilla	0.0109	60	135
PRKY	chrY:7287633-7288958	gorilla	0	286	615
PRKY	chrY:7287633-7288958	human	0.0001	936	1332
PRKY	chrY:7298612-7299384	chimpanzee	0.0478	558	804
PRKY	chrY:7303614-7305238	bonobo	0.0158	251	355
PRKY	chrY:7303614-7305238	chimpanzee	0.038	218	283
PRKY	chrY:7307951-7308946	bonobo	0.0007	446	522
PRKY	chrY:7307951-7308946	chimpanzee	0	374	522
PRKY	chrY:7317538-7317820	gorilla	0.0215	80	290
PRKY	chrY:7319720-7320002	gorilla	0.0389	1	100
PRKY	chrY:7321549-7321821	bonobo	0.0319	114	183
PRKY	chrY:7323620-7323942	bonobo	0.0066	30	151
PRKY	chrY:7336855-7337148	gorilla	0.0176	97	242
PRKY	chrY:7337159-7337664	bonobo	0.028	1	284
PRKY	chrY:7337159-7337664	chimpanzee	0.028	1	284
PRKY	chrY:7341156-7341892	human	0	339	748
PRKY	chrY:7341156-7341892	chimpanzee	0.001	465	748
PRKY	chrY:7346134-7346840	bonobo	0.0008	1	107
PRKY	chrY:7353876-7354015	human	0.0273	76	138
PRKY	chrY:7353876-7354015	chimpanzee	0.0396	54	139
PRKY	chrY:7354762-7355022	chimpanzee	0.0222	181	266
PRKY	chrY:7361945-7362274	gorilla	0.0161	165	244
PRKY	chrY:7361945-7362274	bonobo	0.0002	1	94
PRKY	chrY:7361945-7362274	chimpanzee	0.0002	1	94
PRKY	chrY:7362356-7362872	gorilla	0.0002	211	496

PRKY	chrY:7363060-7363291	human	0.0015	1	147
PRKY	chrY:7366365-7366795	bonobo	0.0019	31	347
PRKY	chrY:7366365-7366795	chimpanzee	0.0384	18	233
PRKY	chrY:7378878-7379479	gorilla	0.0186	311	491
TBL1Y	chrY:7041288-7041422	human	0.0428	12	71
TBL1Y	chrY:7041288-7041422	bonobo	0.0428	12	71
ZFY	chrY:2979919-2980045	orangutan	0.018	1	76

Selection. We used the CODEML module of PAML (version 4.8) (61) to detect branch-specific differences in the nonsynonymous-to-synonymous rate ratios and to test for positive selection acting on X-degenerate genes (excluding pseudogenes *CYorf15A* and *CYorf15B* (*TXLNGY*)) and ampliconic genes (excluding *VCY* present only in two species) in human, chimpanzee, bonobo, gorilla, Sumatran orangutan, Bornean orangutan, and macaque. Coding sequences of Y-chromosomal genes were retrieved from GENBANK or deciphered in this study and aligned using CLUSTALW (62). The phylogenies were generated with the Neighbor-Joining method (63) (with 1,000 bootstrap replicas) as implemented in MEGA7 (64). First, for each gene, the one-ratio model (assuming the same nonsynonymous-to-synonymous rate ratio ω for the entire tree) was compared with the two-ratio model (assuming that the branch-specific ratio ω_s is different from the background ratio ω_o). When the difference between the two models was significant, this indicated that the synonymous-to-nonsynonymous rate ratio was different for the branch tested. In these cases, to test for positive selection, the model assuming the foreground ratio ω to be fixed at 1 (neutral evolution) was compared against an alternative model with branch-specific ω > 1 (positive selection).

We found a total of eight gene-branch combinations that had foreground nonsynonymous-to-synonymous rate ratio significantly different than the background nonsynonymous-to-synonymous rate ratio (Table SN4B). We observed significantly different nonsynonymous-to-synonymous rate ratios on the chimpanzee and bonobo ancestor than other lineages for three X-degenerate genes (*DDX3Y*, *EIF1AY*, and *PRKY*) and one ampliconic gene (*CDY*). We also detected significantly different nonsynonymous-to-synonymous rate ratios in bonobo for two X-degenerate genes (*DDX3Y* and *EIF1AY*), in chimpanzee for *ZFY*, and in human for *RPS4Y2*. However, none of these ratios was significantly higher than one, providing no evidence for positive selection.

Table SN4C. Gene-branch combinations with significantly higher branch-specific than background nonsynonymous-to-synonymous rate ratio. The *p*-values were obtained by computing a χ^2-distributed Likelihood Ratio Test statistic $\Delta LRT=2\times(lnL_1-lnL_0)$, where lnL_1 is the log likelihood value for the alternative model and lnL_0 is the log likelihood value for the null model). The degrees of freedom were computed as $df = np_1-np_0$, where np_1 is the number of parameters for the alternative model and np_0 is the number of parameters for the null model.

Gene	Branch	Background ω_o	Branch-specific ω_s	P-value for testing $\omega_s > \omega_o$	P-value for testing $\omega_s > 1$
CDY	BC	0.44	3.08	0.02	0.30
DDX3Y	Bonobo	0.19	1.11	0.02	0.54
DDX3Y	BC*	0.18	1.44	0.004	0.48

EIF1AY	Bonobo	0.02	>1 (division by 0)	0.03	0.45
EIF1AY	BC	0.02	>1 (division by 0)	0.03	0.44
PRKY	BC	0.18	1.64	0.03	0.11
RPS4Y2	Human	0.16	>1 (division by 0)	0.0002	1.00
ZFY	Chimpanzee	0.04	>1 (division by 0)	0.04	0.44

*BC: bonobo-chimpanzee common ancestor

Supplemental Note S5. Evolutionary scenarios for palindromes.

Palindrome 4. We used two different approaches to obtain information about the conservation of human and chimpanzee palindromes across great apes. First, we used the multiple sequence alignment of Y chromosome assemblies to obtain the coverage of these palindromes. In the case of P4 we observed 23,175 bp of alignment in the bonobo assembly (**Table S5**). This analysis gave us the percentage of P4 present in bonobo Y assembly, however it did not infer that there is a continuous 23-kb block of palindrome P4 on bonobo Y. P4 could be highly fragmented due to Y chromosome degradation or rearrangements and the multiple sequence alignment can still capture such homologous fragments of the palindromes. The longest blocks in the Y multiple sequence alignment that overlap with P4 are 2-4 kb in length and these alignment blocks included sequences from gorilla and human Ys. In the remaining species, sequences homologous to P4 are mostly represented by gaps. Second, to identify the copy number of P4 homologs present in other species, we used alignments generated with LASTZ (3) based alignments. Non-overlapping 1-kb windows of the assembly were aligned to human P4 using LASTZ. The read depth of windows with >80% identity to P4 was used to estimate the copy number of P4. However, we did not find any 1-kb window in bonobo Y which maps to human palindrome P4 with >80% identity. Since we did not find high-confidence windows aligning to P4 in bonobo, we concluded that it is highly fragmented in this species.

Human and chimpanzee palindromic copy numbers used to build Figure 3B. We first simulated 5 million 101-bp paired-end reads from the chimpanzee Y chromosome (panTro6) using wgsim (https://github.com/lh3/wgsim) and parameters -S 9 -1 101 -2 101. Next, we parsed the left arm sequence of each palindrome and 3 MB of X-degenerate region from human (hg38) Y as reference. We mapped the chimpanzee reads to the parsed human sequences. Using bedtools coverage function, we calculated the average read depth of each palindromic arm and X-degenerate regions. Finally, we obtained the copy number of each palindrome using the read depth of X-degenerate regions as a control. We repeated the same procedure by simulating human reads and parsing chimpanzee palindrome arms. The resulting copy numbers in **Table S7**. In the case of P6, P7 and P8, which are homologous to C19, C18, and C17, respectively, we assumed the copy number to be two in both human and gorilla.

Evolution of sequences homologous to human and chimpanzee palindromes. Using parsimony, for each internal node on the great ape phylogenetic tree, we estimated the copy number of each palindrome based on the copy numbers observed in great ape species (**Table S7**). For example, if the copy number of palindrome P is 1, 2, and 2 in chimpanzee, humans, and gorilla, respectively, then the copy number in the human and chimpanzee common ancestor (HC) could be 1 or 2, because of the lack of consensus. Next, the copy number of P in the common ancestor of chimpanzee, human and gorilla is a consensus of the copy number of P in HC (1 or 2) and gorilla (2), which is 2. Accordingly, we estimated the copy number in **Tables SN5A-B** and below there is a summary for each internal node.

Common ancestor of great apes (GA). In this ancestor, partial sequences of all human and chimpanzee palindromes were present, and P1, P2, P4, P5, P8, C2, C4, and C17 were in a multi-copy state (**Tables SN5A-B**). P3, P6, C1, and C3 might have been in single- or multi-copy state (**Tables SN5A-B**). P7, C5, C18, and C19 were in a single-copy state.

Orangutan. In the orangutan lineage, there was an increase in copy number of P1, P2, P4, P5, C3, and C4 (**Fig. 3A, Table SN5A-B**) and a loss of C3 (≈25% loss in coverage, **Table S6**) and P2 (≈27% loss in coverage, **Table S5**) segments. An alternative explanation is a decrease in copy number for P1, P2, P4, P5, C3, and C4, and a gain of C3 and P2 sequences in the common ancestor of great apes.

Common ancestor of bonobo, chimpanzee, human, and gorilla (BCHG). P3, P6, C1, and C3 might have been in a single- or multi-copy state in the common ancestor of great apes, however, for the BCHG, P3, P6, and C1 were in a multi-copy state (i.e. had at least two copies; **Tables SN5A-B**).

Gorilla. In the gorilla lineage, there is a loss of copy number (~1 copy) for homologs P8 and C17 compared to bonobo and orangutan (**Fig. 3**); the loss in copy number from BCHG to gorilla is consistent between P8 and

C17 (**Tables SN5A-B**), which adds additional confidence to this observation. However in the cases of the other homologs -- P7-C18, and P6-C19 -- the shifts from BCHG to gorilla are not concordant, and the actual difference in copy number is less than half a copy. As a result we do not show these inconclusive changes for P6 and P7 copy number in **Fig. 3B**. There is a gain in copy number for palindrome C3: it might have been in a single- or multi-copy state in the common ancestor of great apes, however in gorilla it is present in two copies. There is a loss of C2 in the gorilla lineage in comparison to bonobo and orangutan (**Fig. 3A**). We observed a loss of segments in C1 (≈15% loss in coverage) and C19 (≈40-60% loss in coverage) in gorilla when compared to other great apes (**Table S6**).

Common ancestor of human, bonobo, and chimpanzee. Palindromes P7 and C5 gained copy numbers, whereas P2 might have been in a single- or multi-copy state (**Tables SN5A-B**).

Human. Palindrome P3 had ≈30-35% of its sequence covered in other great apes (**Table S5**), so we assume that the remaining portion of P3 is human-specific. Humans also lost most of the sequences homologous to palindrome C2.

Common ancestor of bonobo and chimpanzee. This ancestor gained a C2 segment; indeed both bonobo and chimpanzee share 85% coverage of C2 whereas the other great apes cover 20-30% of C2, which implies a *Pan*-genus-specific gain of C2 sequences (**Table S6**). C1 and C5 groups are present in more than two copies in both chimpanzee (1) and bonobo, whereas other species have two or fewer copies of these palindromes (Fig. 3A). In the common ancestor of human, chimpanzee, and bonobo, palindrome P2 might have been in a single- or multi-copy state, however the common ancestor of chimpanzee and bonobo has one copy which implies a loss of P2 in it. The *Pan* genus lost P4; we observe that some sequences homologous to P4 are present in bonobo and chimpanzee Y, however they are degraded and not visible as an alignment on the human and chimpanzee Y dot plot (1). Therefore, we assume that P4 was deleted.

Bonobo. The bonobo lineage lost copies of P6, P7, C18, and C19 (**Fig. 3A, Table SN5A-B**). It also lost segments of C18 (≈30-60% loss in coverage **Table S6**) and P7 (≈60% loss in coverage **Table S5**).

Chimpanzee. The chimpanzee lineage gained copies of P3, P5, C3, and C4. It also gained a segment of C1, a palindrome which has <50% coverage in the other great ape Y chromosomes (**Table S6**).

Table SN5A. Reconstructing human palindrome evolution using maximum parsimony. The values from extant species were taken from Table S7 and rounded to the following numbers of copies: <1.34 => “1”, “1.34-1.66” =>”1-2”, “1.67-2.5” => “2”, “>2.5” => “M” (“more than two”).

	P1	P2	P3[#]	P4	P5	P6	P7	P8
Bonobo	1-2	1-2	1-2	0	2	1-2	1	2
Chimpanzee	1-2	1	M	0	M	2[$]	2[$]	2[$]
BC*	1-2	1	1-2-M	0	2-M	2	1-2	2
Human	2	2	2	2	2	2	2	2
BCH**	2	1-2	2	2	2	2	2	2
Gorilla	2	2	2	2	2	1-2	1	1
BCHG***	2	2	2	2	2	2	1-2	1-2
Orangutan	M	M	1	M	M	1	1	2
GA****	2-M	2-M	1-2	2-M	2-M	1-2	1	2

*Bonobo-chimpanzee common ancestor
**Bonobo-chimpanzee-human common ancestor
***Bonobo-chimpanzee-human-gorilla common ancestor
****Common ancestor of great apes
[$]We conservatively assigned the copy number of P6, P7, and P8 as 2 in chimpanzee because of their known homology with C19, C18, and C17 respectively (1).
[#]We can conservatively assume that P3 became multi-copy in BCHG, but instead it might have been multi-copy in the common ancestor of great apes and lost its multi-copy status in orangutan.

Table SN5B. Reconstructing chimpanzee palindrome evolution using maximum parsimony. The values from extant species were taken from Table S7 and rounded to the following numbers of copies: <1.34 => “1”, “1.34-1.66” =>”1-2”, “1.67-2.5” => “2”, “>2.5” => “M” (“more than two”).

	C1 group	C2 group	C3 group	C4 group	C5 group	C17	C18	C19
Bonobo	M	M	1	1-2	M	2	1	1
Chimpanzee	M	M	M	M	M	2	2	2
BC*	M	M	1-M	1-2-M	M	2	1-2	1-2
Human	2	0	1-2	2	2	2	2	2
BCH**	2-M	M	1	2	2-M	2	2	2
Gorilla	2	M	2	2	1	1	1	1
BCHG***	2	M	1-2	2	1-2-M	1-2	1	1-2
Orangutan	1	M	M	M	1	2	1	1
GA****	1-2	M	1-2-M	2-M	1	2	1	1

*Bonobo-chimpanzee common ancestor

**Bonobo-chimpanzee-human common ancestor

***Bonobo-chimpanzee-human-gorilla common ancestor

****Common ancestor of great apes

[$]We conservatively assigned the copy number of C17, C18, and C19 as 2 in human because of their known homology with P8, P7, and P6 respectively (1).

Supplemental Note S6. Species-specific sequences in bonobo, gorilla and orangutan Y chromosome assemblies.

To identify Y chromosome contigs, we have previously filtered out contigs with >95% sequence homology to female reference. However, the species-specific Y chromosome sequences we identified in bonobo, gorilla, and orangutan might be located within the contigs we retained and might have some degree of homology to the female reference. To understand the nature of species-specific sequences, we mapped them (the ones that were >100 bp in length) to their corresponding female references using BWA-MEM (10). We observed that some of these sequences indeed map to chromosome X and the autosomes with different levels of sequence identity (measured as the number of matches observed in the alignment based on CIGAR string). We differentiated among species-specific sequences that have sequence identity of <50%, 50-79%, 80-98%, and 99-100% to autosomal or X chromosomal sequences (**Table SN6**). The majority of the species-specific sequences in these Y chromosome assemblies did not share high levels of sequence identity to the female reference. The sequences with 99-100% sequence identity could represent misassemblies or recent translocations from autosomes to the Y.

One should keep in mind that the quality and completeness of the female reference assemblies vary for these three great ape species, and this can influence the results. Therefore, it is difficult to identify false positive species-specific sequences and make further biological inferences for these sequences from these data.

Table SN6. Sequence identity of species-specific sequences to the corresponding female reference. The numbers in each cell represent the total length of species-specific sequences with defined percentages of sequence identity to the corresponding female reference. The percentages within each cell are computed with respect to the total length of species-specific sequences as defined in the last column.

Sequence identity to the female reference/ Species	**<50%**	**50-79%**	**80-98%**	**99-100%**	**Total length (bp)**
Bonobo	6,600,780 (70.5%)	633,871 (6.8%)	627,981 (6.7%)	71,174 (0.8%)	9,360,114
Gorilla	988,841 (57.2%)	277,942 (16.1%)	308,964 (17.9%)	102,770 (5.9%)	1,728,186
Orangutan	2,467,310 (73.7%)	290,574 (8.7%)	298,381 (8.9%)	57,742 (1.7%)	3,350,046

Supplemental Note S7. Acquisition of the *VCY* gene family by great ape Y chromosomes.

We speculate that the birth of *VCY* occurred in the common ancestor of human and chimpanzee after P8 palindrome was acquired by the common ancestor of great apes (**Table S5**). *VCY* is present on the human Y according to (2) and has high homology to *VCX*, likely due to X-Y gene conversion (65, 66). Hughes and colleagues (1) suggested that *VCY* (XM_003318999.5) is present on the chimpanzee Y. Because of its high similarity to *VCX*, no RT-PCR primers could be designed to amplify the Y-chromosomal *VCY* in chimpanzee (Jennifer Hughes, personal communication), suggesting the role of gene conversion in sequence homogenization between its X and Y copies. Using human *VCY* as a query, we were unsuccessful in retrieving male-specific *VCY* copies in gorilla, orangutan, and bonobo from our Y chromosome draft assemblies (**Table S3**), as well as using additional datasets (see below). No *VCY* has been previously detected in gorilla using either whole-genome sequencing data from male (4) or testis-specific RNA-Seq datasets (67).

We were unable to recover the full-length Y-specific sequence of *VCY* in Sumatran orangutan. We did not find a full-length copy of *VCY* using short whole-genome sequencing paired-end reads from the Sumatran orangutan male (dataset from BioProject PRJNA587121). In addition, when we aligned the testis RNA-Seq datasets from Sumatran orangutan (dataset from BioProject PRJNA587121) and Bornean orangutan (dataset from BioProject PRJNA587108), the consensus sequence retrieved from the RNA-Seq reads had the highest similarity to the X-chromosomal *VCX* copy. Additionally, the male-specific gene sequence of *VCY* was previously reported to be missing from Bornean orangutan (Cortez et al. 2014), based on the analysis of whole-genome sequencing data.

We were unable to recover the full-length Y-specific sequences of *VCY* in bonobo. Currently the full-length male-specific *VCY* gene sequence is unavailable for chimpanzee, the closest relative to bonobo. When we aligned the whole-genome bonobo male reads (this study) to the human protein-coding *VCY* sequence (CCDS56617.1) as reference, the consensus sequence reconstructed from these reads had the highest similarity to the *VCX* 3B-like gene copies in chimpanzee and bonobo. Consistently, when we aligned the testis RNA-Seq data from bonobo (dataset from BioProject PRJNA587108) to the human *VCY*, the consensus sequences retrieved from the aligned RNA-Seq reads also had the highest similarity to the *VCX* 3B-like gene copies in chimpanzee and bonobo. It is possible though that the *VCY* copy could not be detected in bonobo because of its high sequence similarity to the X-chromosomal copy, which is the case for chimpanzee.

Our data are consistent with the birth of *VCY* ~6-7 million years ago in the human-chimpanzee common ancestor (Figure 2) potentially due to gene conversion with its homologue on the X chromosome, *VCX*. *VCX* was detected via low-stringency hybridization only in simian primates (68). This fact and the notion that *VCY* is located in the Y-added region acquired by the human Y chromosome 30-40 million years ago (69) led to an alternative hypothesis that both *VCX* and *VCY* were already present in the common ancestor of simians (69, 70), but then *VCY* was lost (or degraded beyond sequence similarity recognition) in multiple independent primate lineages.

Supplemental Tables

Table S1. The statistics for *de novo* bonobo, gorilla, and orangutan Y chromosome assemblies and for the human and chimpanzee reference Y chromosomes (1, 2).

Species	Assembly length including non-ambiguous base pairs (non-Ns, Mb) + ambiguous base pairs (Ns, in Mb)	NG50[1] (in bp, using G=8.5 Mb)	N50[2] (in bp)	Number of scaffolds
Orangutan	16.1 + 1.3	1,388,499	773,523	1,178
Gorilla	14.3 + 0.008	150,017	95,534	268
Bonobo	22.6 + 0.8	153,556	32,114	3,590
Chimpanzee[1]	25.3 + 1.1	-	-	1
Human[2]	23.6 + 33.6[3]	-	-	1

[1]NG50: the size of the scaffold for which half of the conserved X-degenerate regions (set to genome size G=8.5 Mb based on estimates in human (2)) is in scaffolds that are equal to or larger than this size.
[2]N50: the size of the scaffold for which half of the assembly is in scaffolds that are equal to or larger in size.
[3]Includes long heterochromatic array on the long arm of the Y chromosome

Table S2. Alignment statistics.

(A) Portion of a species' Y chromosome assembly aligning to each other species, in PROGRESSIVECACTUS (18) multi-species alignments. Percentage shown is the portion of bases in the column-species Z that has any pairwise alignment to the row-species W. Denominator is the non-N count of the column-species Z. **(B)** Portion aligning to each other species, in LASTZ (3) pairwise alignments. **(C)** Average identity in PROGRESSIVECACTUS (18) alignment blocks containing all five species. **(D)** Average identity in LASTZ (3) pairwise alignments.

A. Portion of a species aligning to each other species, in **PROGRESSIVECACTUS multi-species** alignments.

proportion of / aligning to	Human Y	Chimpanzee Y	Bonobo Y	Gorilla Y	Orangutan Y
Human Y	—	77.15%	47.45%	75.45%	63.32%
Chimpanzee Y	66.61%	—	52.74%	66.76%	61.12%
Bonobo Y	61.76%	82.78%	—	64.83%	57.98%
Gorilla Y	57.42%	58.40%	36.82%	—	52.82%
Orangutan Y	55.47%	63.30%	38.73%	61.26%	—

B. Portion aligning to each other species, in **LASTZ pairwise** alignments.

proportion of / aligning to	Human Y	Chimpanzee Y	Bonobo Y	Gorilla Y	Orangutan Y
Human Y	—	92.14%	64.59%	89.61%	86.40%
Chimpanzee Y	84.26%	—	65.58%	85.19%	85.85%
Bonobo Y	84.05%	96.00%	—	86.50%	85.34%
Gorilla Y	78.21%	83.22%	56.05%	—	79.45%
Orangutan Y	75.53%	83.57%	55.67%	79.44%	—

C. Average identity in **PROGRESSIVECACTUS multi-species** alignment blocks containing all five species.

identity of / aligning to	Human Y	Chimpanzee Y	Bonobo Y	Gorilla Y	Orangutan Y
Human Y	—	97.89%	97.84%	97.18%	93.74%
Chimpanzee Y	97.89%	—	99.20%	96.97%	93.59%
Bonobo Y	97.79%	99.14%	—	96.88%	93.47%
Gorilla Y	97.18%	96.97%	96.93%	—	93.55%
Orangutan Y	93.61%	93.46%	93.38%	93.42%	—

D. Average identity in **LASTZ pairwise** alignments.

identity of / aligning to	Human Y	Chimpanzee Y	Bonobo Y	Gorilla Y	Orangutan Y
Human Y	—	95.76%	95.58%	95.81%	92.47%
Chimpanzee Y	95.60%	—	97.84%	94.53%	91.95%
Bonobo Y	95.19%	98.27%	—	94.30%	91.83%
Gorilla Y	95.01%	93.99%	93.98%	—	91.85%
Orangutan Y	92.46%	91.91%	92.28%	92.71%	—

Table S3. The estimated number of substitutions (after correcting for multiple hits).
(**A**) between gorilla and chimpanzee, and between gorilla and human; (**B**) between gorilla and bonobo, and between gorilla and human, considering autosomes and Y chromosome separately, with corresponding χ^2 statistics and *p*-value showing an elevation in the *Pan* lineage. We used a test similar to the relative rate test used in (22). The last column shows the alignment length.

A

Autosomes	**N subst. gorilla -> chimp**	**N subst. gorilla -> human**	**Increase in N subst.**	**Difference from ratio of 1 χ^2, *p*-value**	**Alignment length**
	40,594,903	40,364,251	0.6%	657.1; $<1\times10^{-5}$	2,306,528,605 bp
Y	**N subst. gorilla -> chimp**	**N subst. gorilla -> human**	**Increase in N subst.**	**χ2**	**Alignment length**
	148,651	137,763	7.9%	414; $<1\times10^{-5}$	4,734,119 bp

B

Autosomes	**N subst. gorilla -> bonobo**	**N subst. gorilla -> human**	**Increase in N subst.**	**Difference from ratio of 1 χ^2, *p*-value**	**Alignment length**
	41,517,515	40,364,251	2.9%	16,243.7; $<1\times10^{-5}$	2,306,528,605 bp
Y	**N subst. gorilla -> bonobo**	**N subst. gorilla -> human**	**Increase in N subst.**	**χ2**	**Alignment length**
	151,018	137,763	9.6%	608.6; $<1\times10^{-5}$	4,734,119 bp

Table S4. Gene birth and death rates (in events per millions of years) on the Y chromosome of great apes, as predicted using the Iwasaki and Takagi gene reconstruction model (33).

BC - common ancestor of bonobo and chimpanzee; BCH - common ancestor of bonobo, chimpanzee, and human; BCHG - common ancestor of bonobo, chimpanzee, human, and gorilla. GA - common ancestor of great apes.

	X-degenerate genes		Ampliconic genes	
Branch	**Birth rate**	**Death rate**	**Birth rate**	**Death rate**
Bonobo-BC	1.00×10^{-4}	1.00×10^{-4}	1.00×10^{-4}	0.182
Chimpanzee-BC	1.00×10^{-4}	8.00×10^{-2}	1.00×10^{-4}	1.00×10^{-4}
Human-BCH	1.90×10^{-5}	1.90×10^{-5}	1.90×10^{-5}	1.90×10^{-5}
Gorilla-BCHG	1.43×10^{-5}	1.43×10^{-5}	1.43×10^{-5}	1.43×10^{-5}
Orangutan-GA	7.14×10^{-6}	2.06×10^{-2}	7.14×10^{-6}	7.14×10^{-6}
Macaque-Root	3.45×10^{-6}	3.45×10^{-6}	3.45×10^{-6}	9.92×10^{-3}
BC-BCH	2.35×10^{-5}	4.89×10^{-2}	2.35×10^{-5}	9.54×10^{-2}
BCH-BCHG	5.71×10^{-5}	5.71×10^{-5}	5.71×10^{-2}	5.71×10^{-5}
BCHG-GA	1.43×10^{-5}	1.43×10^{-5}	1.43×10^{-5}	1.43×10^{-5}
GA-Root	6.67×10^{-6}	4.04×10^{-3}	6.67×10^{-6}	6.67×10^{-6}

Table S5. The sequence coverage (percentage) of human palindromes P1-8 (arms) by non-human great ape Y assemblies.

The repeats annotated by REPEATMASKER (19) were excluded from the calculations.

Human palindrome	Length, bp					Coverage, percentage			
	Chimpanzee	Bonobo	Gorilla	Orangutan	Human*	Chimpanzee	Bonobo	Gorilla	Orangutan
P1	362334	340526	332205	248261	608650	59.53	55.95	54.58	40.79
P2	50349	50104	49059	29283	76387	65.91	65.59	64.22	38.34
P3	64644	62144	66195	55353	179793	35.95	34.56	36.82	30.79
P4	77198	75075	83143	71380	93979	82.14	79.88	88.47	75.95
P5	159451	158556	157154	144102	166929	95.52	94.98	94.14	86.33
P6	35529	35461	34532	32762	36832	96.46	96.28	93.76	88.95
P7	4439	1134	4385	4134	5414	81.99	20.95	80.99	76.36
P8	15027	13698	12688	12783	16728	89.83	81.89	75.85	76.42
Total	768971	736698	739361	598058	1184712	64.91	62.18	62.41	50.48

*Palindrome arm length

Table S6. The sequence coverage (percentage) of chimpanzee palindromes C1-19 (arms) across great apes.

The repeats annotated by REPEATMASKER (19) were excluded from the calculations. The palindromes were clustered into five homology groups: C1 (C1+C6+C8+C10+C14+C16), C2 (C2+C11+C15), C3 (C3+C12), C4 (C4+C13), and C5 (C5+C7+C9). The numbers in bold represent the palindrome with highest coverage within each group, which we used as the representative coverage of that homology group.

Chimpanzee palindrome	Length, bp					Coverage, percentage			
	Human	Bonobo	Gorilla	Orangutan	Chimpanzee*	Human	Bonobo	Gorilla	Orangutan
C1	36753	34093	26042	37977	66916	**54.92**	**50.95**	**38.92**	**56.75**
C2	35250	111606	27889	37715	141680	24.88	78.77	19.68	26.62
C3	59088	59534	57163	38502	82274	**71.82**	**72.36**	**69.48**	**46.80**
C4	119921	120443	119334	113771	127172	**94.30**	**94.71**	**93.84**	**89.46**
C5	114414	113276	114951	110056	136579	**83.77**	**82.94**	**84.16**	**80.58**
C6	15973	15175	6546	17314	58166	27.46	26.09	11.25	29.77
C7	45587	45683	45871	45208	137290	33.20	33.27	33.41	32.93
C8	21757	20813	12420	22938	64725	33.61	32.16	19.19	35.44
C9	46790	47279	47564	46658	139044	33.65	34.00	34.21	33.56
C10	16031	15292	6855	17332	59322	27.02	25.78	11.56	29.22
C11	24325	105428	27824	37285	123692	19.67	85.23	22.49	30.14
C12	46915	47591	46387	27052	76418	61.39	62.28	60.70	35.40
C13	117820	118341	117201	112189	132034	89.23	89.63	88.77	84.97
C14	20723	20088	11676	21965	47853	43.31	41.98	24.40	45.90
C15	23119	95113	25497	35465	111841	**20.67**	**85.04****	**22.80**	**31.71**
C16	40857	32673	30231	41750	76391	53.48	42.77	39.57	54.65
C17	15364	15072	12961	12978	17516	**87.71**	**86.05**	**74.00**	**74.09**
C18	6686	2582	4741	6304	6888	**97.07**	**37.49**	**68.83**	**91.52**
C19	155497	155916	56993	122994	168341	**92.37**	**92.62**	**33.86**	**73.06**
Total	962870	1175998	798146	905453	637282	54.27	66.29	44.99	51.04

*Palindrome arm length

**In the case of cluster C2, different palindromes had highest coverage for different species and we considered C15 as a representative because it had the highest coverage for more than one species, while other palindromes had highest coverage for only one species.

Table S7. The copy number for sequences homologous to (A) human and (B) chimpanzee palindromes.

The numbers for bonobo, gorilla, and orangutan were obtained based on median read depth of 1-kb windows homologous to human or chimpanzee palindromes. The copy number for chimpanzee and human were obtained by examining the dotplot of human and chimpanzee Y(1). In brackets, we indicate the known homologs of chimpanzee and human palindromes in human and chimpanzee, respectively (1). To validate the accuracy of this approach, we used simulated reads to estimate copy number for the human (P1-5) and chimpanzee (C1-5) palindromes (Note S5). The resulting estimates were similar to those presented in the literature (2, 71). In the case of P6, P7 and P8, which are homologous to C19, C18, and C17, respectively, we assumed the copy number to be two in both human and chimpanzee.

A

Palindrome/ Species	P1	P2	P3*	P4	P5	P6	P7	P8
Human	2	2	2	2	2	2	2	2
Chimpanzee	1.65 (C3+C4)	1.12 (C3)	3.46 (C1 parts)	0	3.5 (C4)	2 (C19)	2 (C18)	2 (C17)
Bonobo	1.64	1.46	1.62	0	2.13	1.42	0.70	1.98
Gorilla	1.99	1.99	1.69	2.49	1.91	1.4	1.23	0.88
Orangutan	6.52	13.13	1.05	5.67	7.29	1.06	1.04	1.80

*Note: We assume that some parts of human palindrome P3 in chimpanzee are multi-copy (those that share homology with C1), while others are single-copy.

B

Palindrome/ Species	C1 group	C2 group	C3 group	C4 group	C5 group	C17	C18	C19
Human	1.94 (P3 parts)	0	1.47 (P1, P2)	2.06 (P5, P1)	2.13	2 (P8)	2 (P7)	2 (P6)
Chimpanzee	>2	>2	>2	>2	>2	2	2	2
Bonobo	13.29	8.42	1.18	1.41	9.31	2.27	0.80	1.25
Gorilla	1.87	2.54	2.01	2.04	1.12	0.93	1.27	1.26
Orangutan	1.02	6.07	12.13	7.85	1.07	1.87	1.02	1.02

Table S8. Summary of Y chromosome species-specific sequences.

The copy number of species-specific blocks in multi-species alignments. Only >100-bp blocks were analyzed to compute the percentages (shown in parentheses) from the total species-specific sequence. CN - copy number.

Species	Total length	In blocks with CN≤1.33 (i.e. CN≈1)	In blocks with 1.34<CN≤1.66 (CN between 1 and 2, uncertain)	In blocks with 1.67<CN≤2.5 (i.e. CN≈2)	In blocks with CN>2.5 (i.e. CN>2)
Bonobo	9,360,114 bp	1,148,427 bp (12.27%)	628,997 bp (6.72%)	1,670,778 bp (17.85%)	5,911,912 bp (63.16%)
Gorilla	1,728,186 bp	725,417 bp (41.98%)	249,531 bp (14.44%)	245,589 bp (14.21%)	507,649 bp (29.37%)
Orangutan	3,350,046 bp	2,175,864 bp (64.95%)	158,549 bp (4.73%)	154,780 bp (4.62%)	860,853 bp (25.69%)

Table S9. The number of observed chromatin contacts, followed by the chromatin interactions weighted by their probability (multi-mapping reads are allocated probabilistically (46)).

The density of chromatin interactions is higher in palindromes. The table is based on human iPSC data (47). See also Fig. S8.

HUMAN	total number of chromatin interactions	weighted number of chromatin interactions	region length [Mb]	**density of weighted interactions [per Mb]**
palindrome interactions	82,619	14,362	6	**2,489**
mixed interactions	70,533	12,111	-	-
other interactions	181,178	26,064	24	**1,086**
sum	334,330	52,536	30	

Table S10. The generated-here and previously unpublished sequencing datasets used for assembly generation and classification, including their summary information.
Sequencing data are available under BioProject PRJNA602326.

Species	Read type	Source	Individual ID	Insert size (bp)	Read count	Read length (bp)	Sequencing technology	SRA accession numbers
Bonobo	paired-end	Whole-genome	PR00251	1,000	319,637,420	251	Illumina HiSeq2500	SRR11032812
Bonobo	mate-pair	Whole-genome	PR00251	8,000	120,181,539	100	Illumina HiSeq2500	SRR11032813
Bonobo	long reads	Y flow-sorted	Ppa_MFS	>7,000	818,697	variable	PacBio	SRR11032811, SRR11032810, SRR11032809, SRR11032808
Orangutan	paired-end	Whole-genome	1991-0051	1,000	303,928,291	251	Illumina HiSeq2500	SRR11032815
Orangutan	synthetic long reads	Whole-genome	AG06213	~350 bp	437,361,894	151	10X Genomics	SRR11039028, SRR11032816, SRR11039026, SRR11039027
Orangutan	mate-pair	Whole-genome	1991-0051	8,000	120,384,643	151	Illumina HiSeq2500	SRR11032814
Gorilla	paired-end	Whole-genome	KB3781	550 bp	120,740,133	150	NextSeq	SRR11032807

*Before any trimming, adapter removal or quality filtering. For paired reads, the number of read pairs is listed.

Table S11. The number of variants before and after the polishing step.

The haploid variants reported by FREEBAYES (14) were filtered to retain only high quality calls (QUAL≥ 30). The polishing step reduces the number of variants present in the assembly.

ORANGUTAN	Before the polishing	After the polishing
All called variants	294,544	286,782
Called variants with QUAL≥30	38,597	4,537
BONOBO	Before the polishing	After the polishing
All called variants	414,617	408,580
Called variants with QUAL≥30	52,158	5,318

Table S12. The coordinates of palindromes on panTro6 and hg38 Y chromosome.

The coordinates were obtained from (4) and updated to the current version of chimpanzee Y, panTro6.

A

Palindrome	Start	End	The end of left arm (approximated)
P1	23359067	26311550	24822577
P2	23061889	23358813	23208197
P3	21924954	22661453	22208730
P4	18450291	18870104	18640356
P5	17455877	18450126	17951255
P6	16159590	16425757	16269541
P7	15874906	15904894	15883575
P8	13984498	14058230	14019652

B

Chimpanzee palindrome	Start	End	Amplicon color following (1)	Approximate arm length (half of palindrome)	The end of left arm (approximated)
C1	1759451	2,053,069	Pink	146809	1906260
C2	2298081	2,984,818	Blue	343368.5	2641450
C3	3587737	3,925,944	Red	169103.5	3756841
C4	4669973	5,444,881	Gold	387454	5057427
C5	8651546	9,099,775	Turquoise	224114.5	8875661
C6	9099776	9,383,863	Pink	142043.5	9241820
C7	9383864	9,832,093	Turquoise	224114.5	9607979
C8	9832094	10,116,181	Pink	142043.5	9974138
C9	10116182	10,564,411	Turquoise	224114.5	10340297
C10	10564412	10,851,248	Pink	143418	10707830
C11	11060051	11,674,261	Blue	307105	11367156
C12	12651797	12,963,129	Red	155666	12807463
C13	13340000	14,084,660	Gold	372330	13712330
C14	14798116	15,024,316	Pink	113100	14911216
C15	15493746	16,056,815	Blue	281534.5	15775281
C16	16477310	16,791,733	Pink	157211.5	16634522
C17	21591500	21,671,300		39900	21631400
C18	23517939	23,546,819		14440	23532379
C19	23807052	24,577,396		385172	24192224

Table S13. The list of ENCODE datasets analyzed in the search for regulatory elements in P6 and P7.

To identify regulatory regions in P6 and P7, we downloaded following bam files from the ENCODE portal (https://www.encodeproject.org/; Date accessed: Sept 20, 2019) with the identifiers: ENCSR000ALB, ENCSR000AKL, ENCSR000ALG, ENCSR000EOQ, ENCSR112ALD, ENCSR136ZQZ, ENCSR956VQB, ENCSR215WNN, and ENCSR729DRB.

Experiment	Unfiltered BAM	Target	Tissue	Link
ENCSR000ALB	ENCFF735TGN	H3K27Ac	HUVEC	https://www.encodeproject.org/experiments/ENCSR000ALB/
ENCSR000AKL	ENCFF322MOQ	H3K4me1	HUVEC	https://www.encodeproject.org/experiments/ENCSR000AKL/
ENCSR000ALG	ENCFF261CBZ	Control	HUVEC	https://www.encodeproject.org/experiments/ENCSR000ALG/
ENCSR000EOQ	ENCFF042VZB	Dnase-seq	HUVEC	https://www.encodeproject.org/experiments/ENCSR000EOQ/
ENCSR112ALD	ENCFF319GEZ	CREB1	HepG2	https://www.encodeproject.org/experiments/ENCSR112ALD/
ENCSR136ZQZ	ENCFF807LQS	H3K27Ac	Testis	https://www.encodeproject.org/experiments/ENCSR136ZQZ/
ENCSR956VQB	ENCFF077NRU	H3k4me1	Testis	https://www.encodeproject.org/experiments/ENCSR956VQB/
ENCSR215WNN	ENCFF511LQO	Control	Testis	https://www.encodeproject.org/experiments/ENCSR215WNN/
ENCSR729DRB	ENCFF639PHQ	Dnase-seq	Testis	https://www.encodeproject.org/experiments/ENCSR729DRB/

Supplemental Figures

Figure S1. Flowcharts for the assemblies of (A) bonobo, (B) Sumatran orangutan, and (C) gorilla.

Blue: input datasets, green: software tools, pink: processed datasets.

A. Bonobo

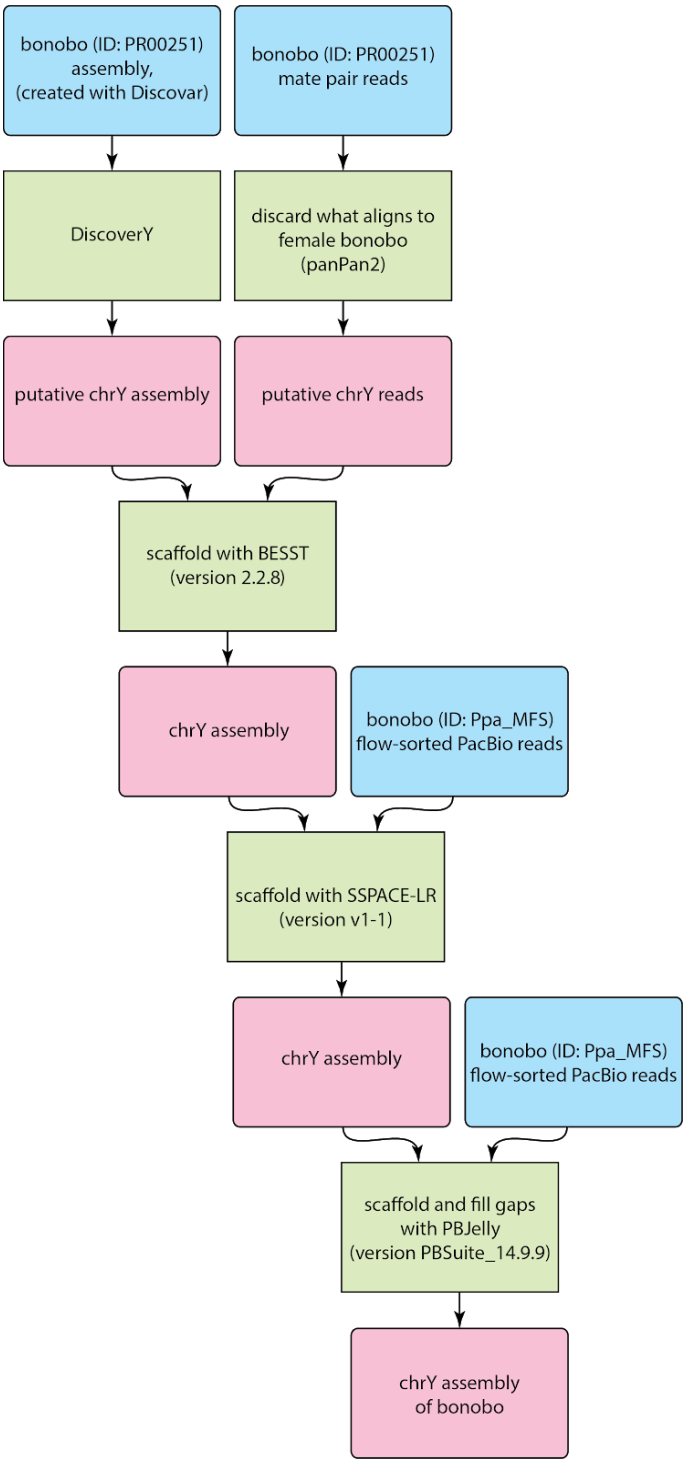

B. Sumatran orangutan

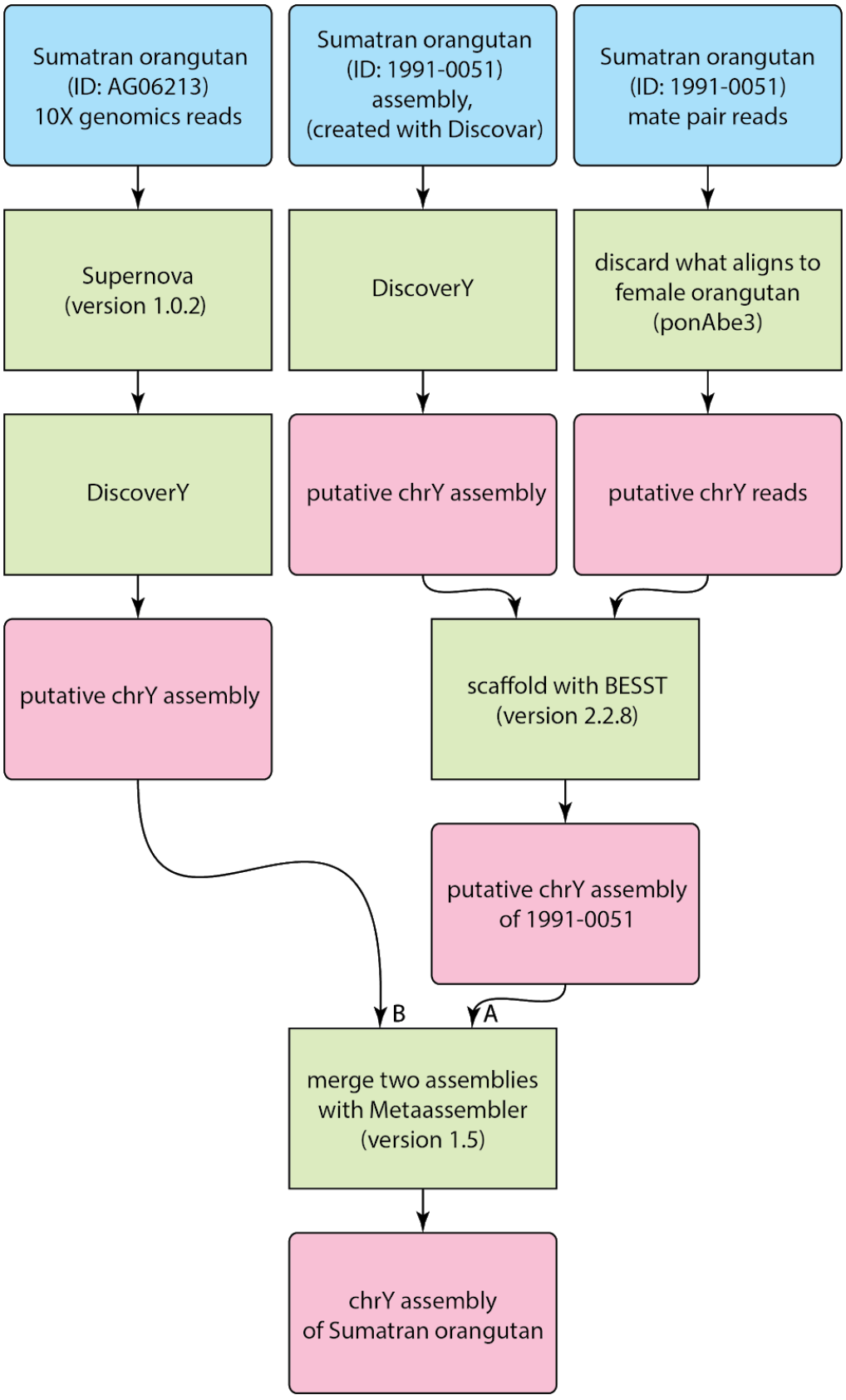

C. Gorilla

The accession numbers are GCA_900199665 and GCA_001484535.2, for Warris et al. (5), and Tomaszkiewicz et al. (4) assemblies, respectively.

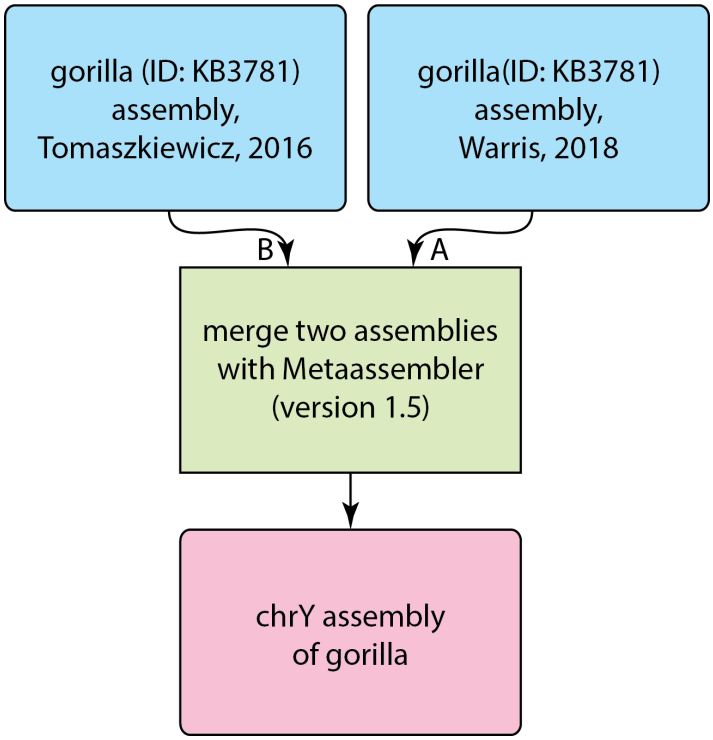

Figure S2. A comparison of bonobo, gorilla and orangutan Y chromosome assemblies against (A) the human Y reference assembly (hg38) and (B) the chimpanzee Y reference assembly (panTro6).

The scaffolds in each assembly were ordered to match (A) the human Y chromosome, or (B) the chimpanzee Y chromosome, using MAUVE (72) v.2015-02-25. This served as a quality control; the limited continuity of the assemblies currently does not allow for the detection of structural rearrangements. The heterochromatic portion of the *q* arm of the human Y chromosome was omitted. Dot plots were generated with GEPARD v.1.40 (36) using word length 50. This ordering of scaffolds was used only to check for assembly completeness and is not used in the rest of the paper.

A

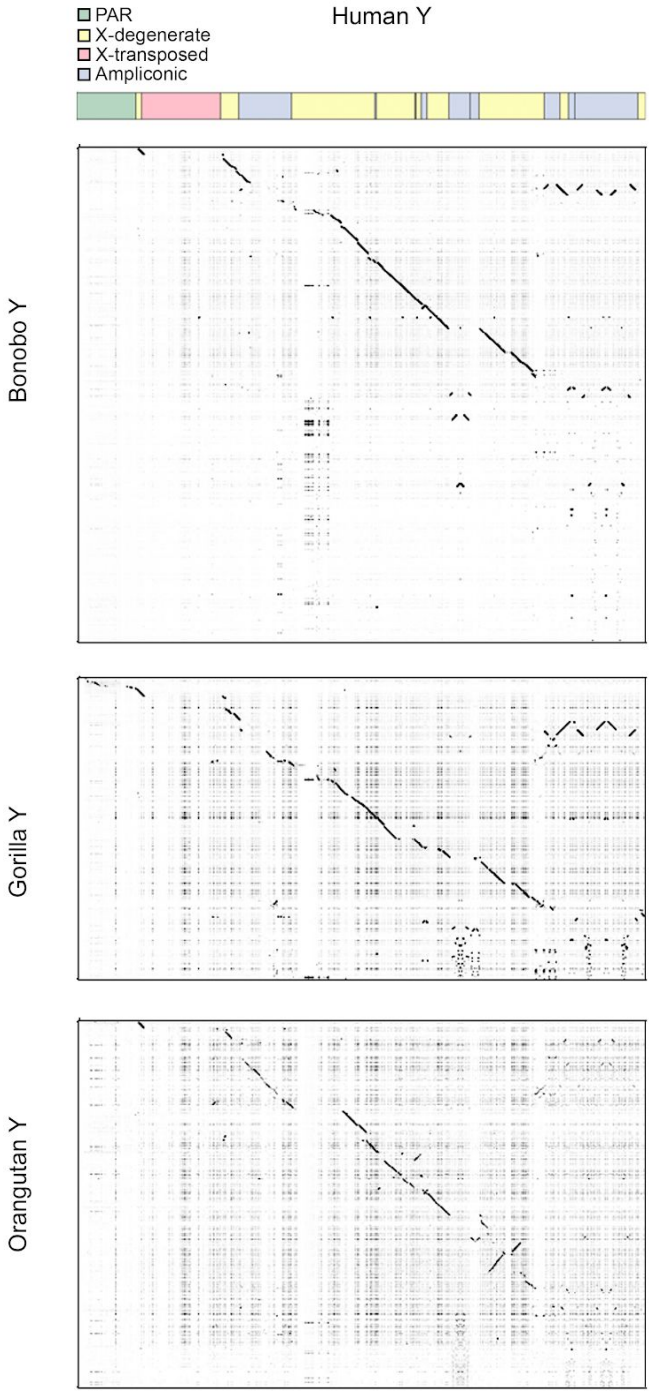

B

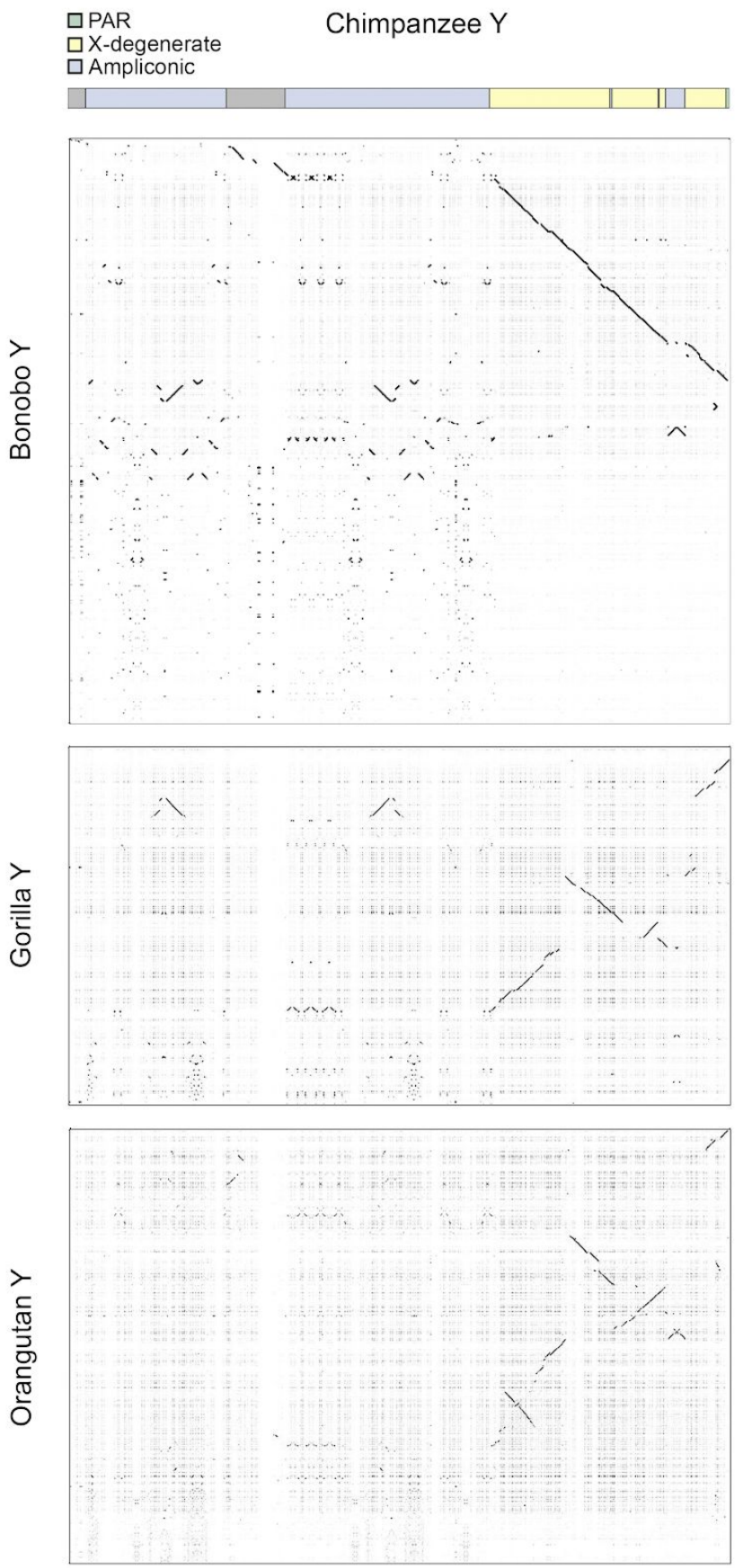
PAR
X-degenerate
Ampliconic
Chimpanzee Y
Bonobo Y
Gorilla Y
Orangutan Y

Figure S3. Protein-coding gene sequence retrieval in the new Y assemblies.
(A) For evaluation purposes, we aligned the scaffolds from each of bonobo, Sumatran orangutan and gorilla Y chromosome assemblies to species-specific or closest-species-specific reference coding sequences using BWA-MEM (v.0.7.10) (10). Next, we visualized the alignment results in Integrative Genomics Viewer (IGV) (v.2.3.72). Consensus sequences were retrieved to evaluate sequence coverage over the reference sequence (in percentage) using BLAST (31). The results were represented as heatmaps using pheatmap package in R.
(B) Table of accession numbers used as queries.

A

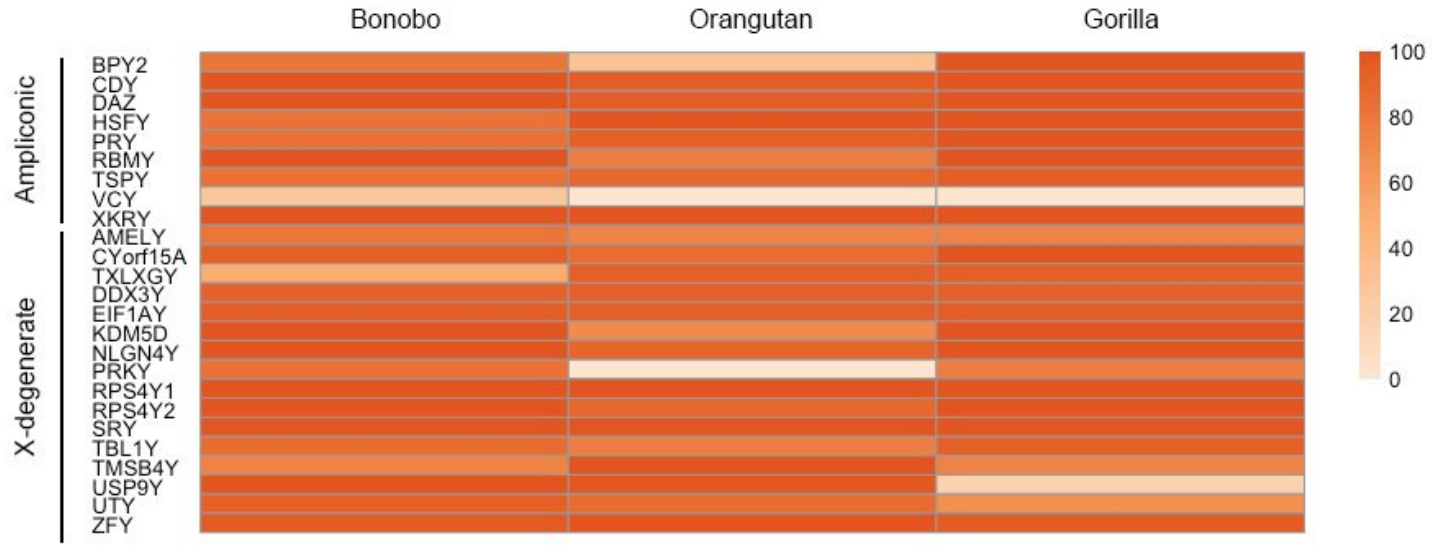

B

Coding sequence	Bonobo	Orangutan	Gorilla
BPY2	AY958084.1	KP141770.1	GATR01000016.1
CDY	AY958081.1	KP141772.1	GATR01000022.1
DAZ	AY958083.1	KP141773.1	GATR01000021.1
HSFY	CCDS35475.1	KP141774.1	GATR01000004.1
PRY	CCDS14799.1	KP141776.1	GATR01000017.1
RBMY	AH014838.2	KP141777.1	GATR01000007.1
TSPY	AY958082.1	KP141780.1	GATR01000012.1
VCY	XM_003318999.5	CCDS56617.1	CCDS56617.1
XKRY	NM_004677.2	NM_004677.2	NM_004677.2
AMELY	NM_001102459.1	ENST00000215479.10	FJ532255.1
CYorf15A	AY633113.1	NR_045128.1	FJ532256.1

TXLNGY	NR_045129.1	GATK01000021.1	FJ532257.1
DDX3Y	AY633112.1	NM_001131248.1	FJ532258.1
EIF1AY	AY633115.1	GATK01000002.1	FJ532259
KDM5D	AY736376.1	GATK01000003.1	FJ532260.1
NLGN4Y	AY728015.1	KP141775.1	FJ532261
PRKY	AY728014.1	ENST00000533551.5	FJ532262
RPS4Y1	AY633110.1	GATK01000004.1	FJ532263.1
RPS4Y2	AY633111.1	KP141778.1	FJ532264
SRY	AY679780.1	KP141779.1	X86382.1
TBL1Y	ENST00000383032.6	GATK01000018.1	FJ532265
TMSB4Y	ENST00000284856.4	GATK01000007.1	FJ532266
USP9Y	ENST00000338981.7	GATK01000005.1	FJ532267
UTY	AY679781.1	GATK01000020.1	FJ532268.1
ZFY	AY679779.1	GATK01000006.1	AY913764

Figure S4. (A, C, E, G, I) Thresholds used for classification of windows into X-degenerate versus ampliconic, and (B, D, F, H, J) average copy number for overlapping 5-kb windows.

X-degenerate windows are shown in yellow, whereas ampliconic windows are shown in blue (or turquoise).

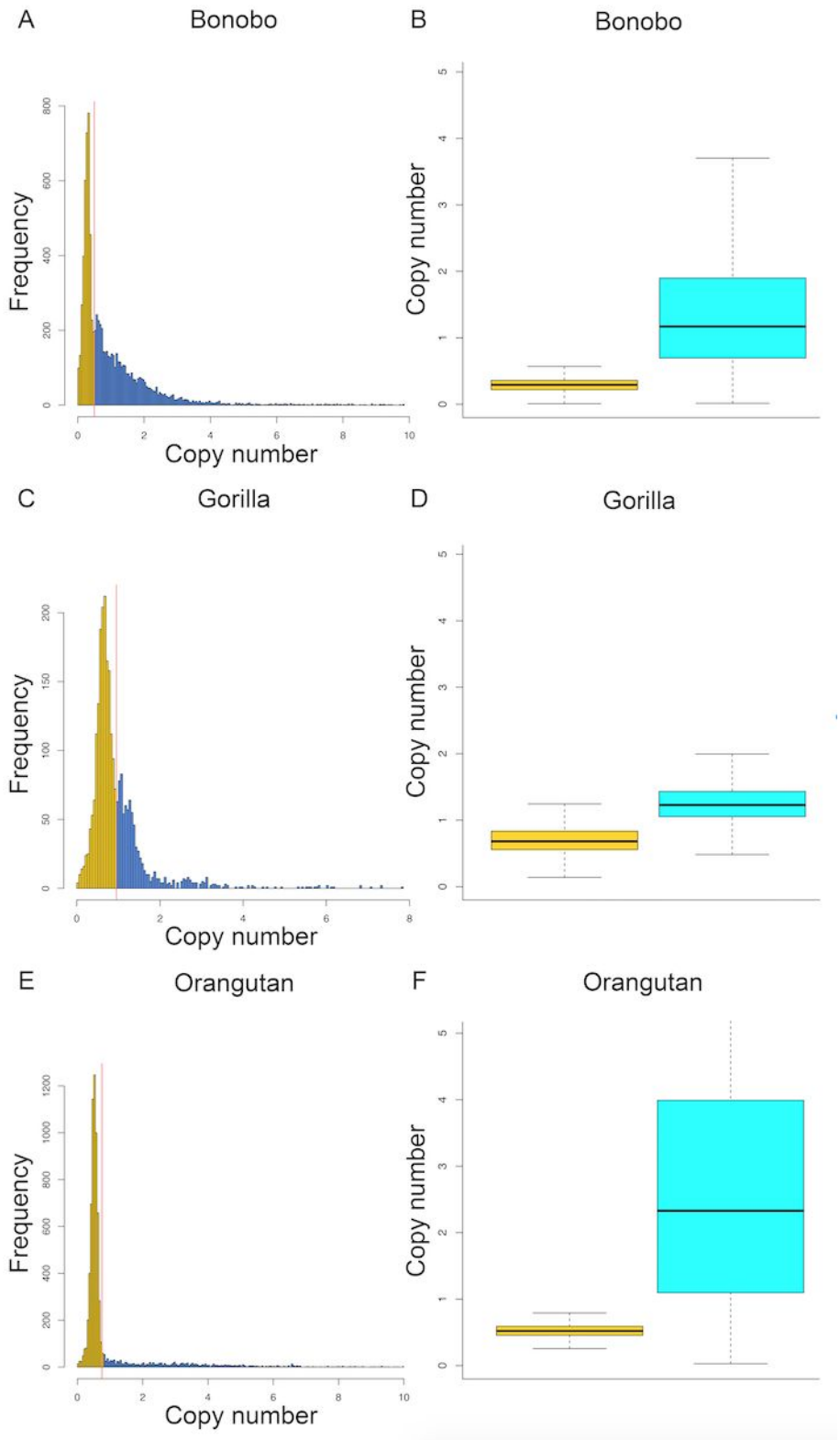

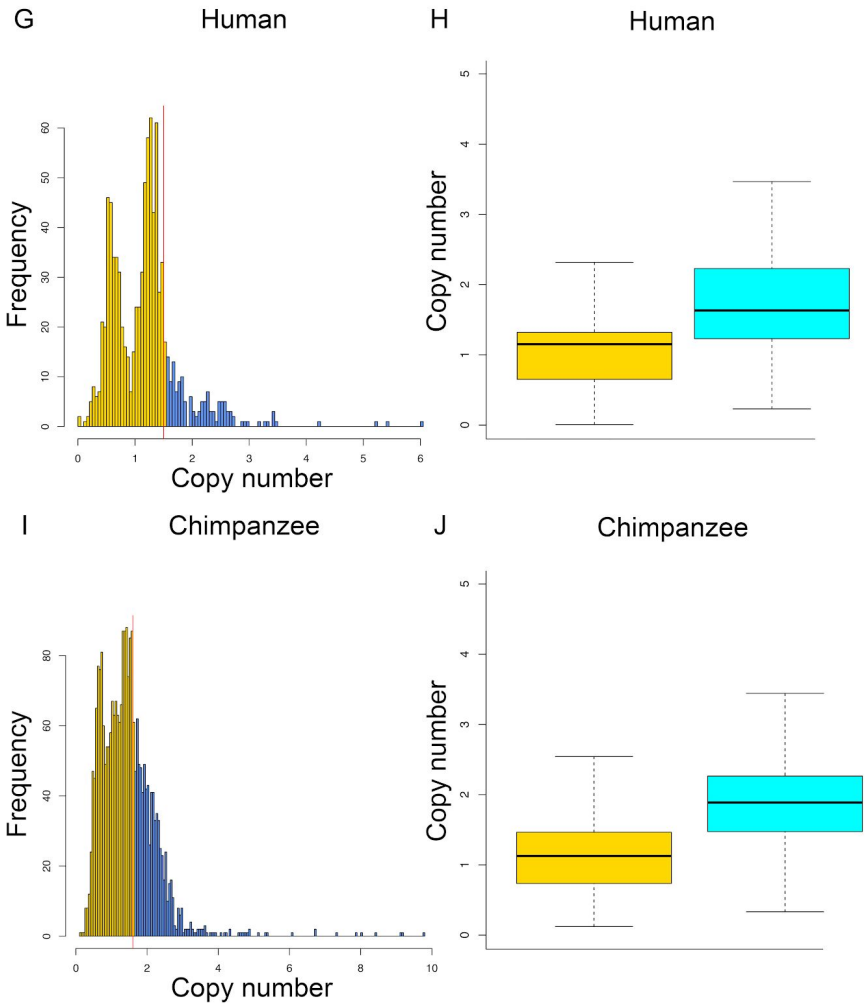
G
Human
Frequency
Copy number
H
Human
Copy number
I
Chimpanzee
Frequency
Copy number
J
Chimpanzee
Copy number

Figure S5. Shared and lineage-specific sequences in multi-species alignments.

Counts of aligned bases in each set of species. For example, the first five bars reflect alignments involving human, chimpanzee, bonobo, gorilla, and orangutan; the sixth through ninth bars reflect alignments involving human, chimpanzee, bonobo, and gorilla but not orangutan, etc.; the last five columns reflect species-specific sequences.

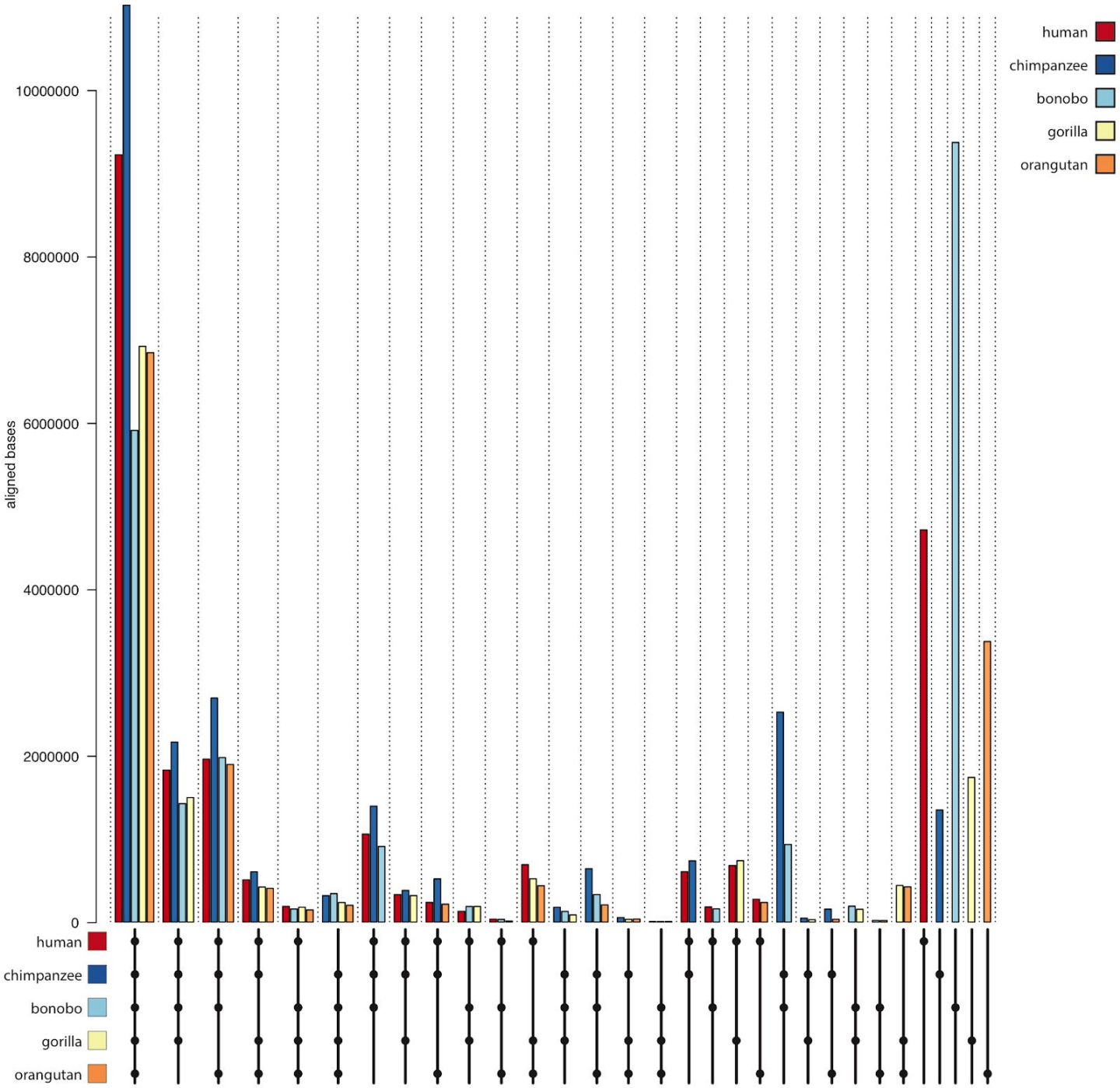

Figure S6. Reconstructed gene content of great apes.

The first six rows have information about the gene content of great apes and macaque, which were used as an input for the model of Iwasaki and Takagi (33). The other rows were reconstructed by the model. BC - common ancestor of bonobo and chimpanzee; BCH - common ancestor of bonobo, chimpanzee, and human; BCHG - common ancestor of bonobo, chimpanzee, human, and gorillas. GA - common ancestor of great apes. We defined the presence of *RPS4Y2* and *MXRA5Y* in bonobo and orangutan based on AUGUSTUS, and Y chromosome specific testis transcriptome assembly results (29). The presence of *RPS4Y2* gene was confirmed in bonobo through gene prediction (shares 100% identity with chimpanzee *RPS4Y2*) and assembled transcript sequences (shares 99.6% identity with chimpanzee *RPS4Y2*). *MXRA5Y*, which is psedogenized in human and chimpanzee (71), was missing in orangutan (no gene prediction or transcript found) and pseudogenized in bonobo (gene prediction annotated as X chromosome homolog *MXRA5* and missing the first three exons of *MXRA5* in its sequence). In the case of gorilla, we did not find its transcript in transcriptome assembly and a BLAT search of human *MXRA5Y* gene (NC_000024.10:11952465-11993293) resulted in a 12-kb long hit which is around 20% of the gene. We assumed the gene is lost in gorilla as well.

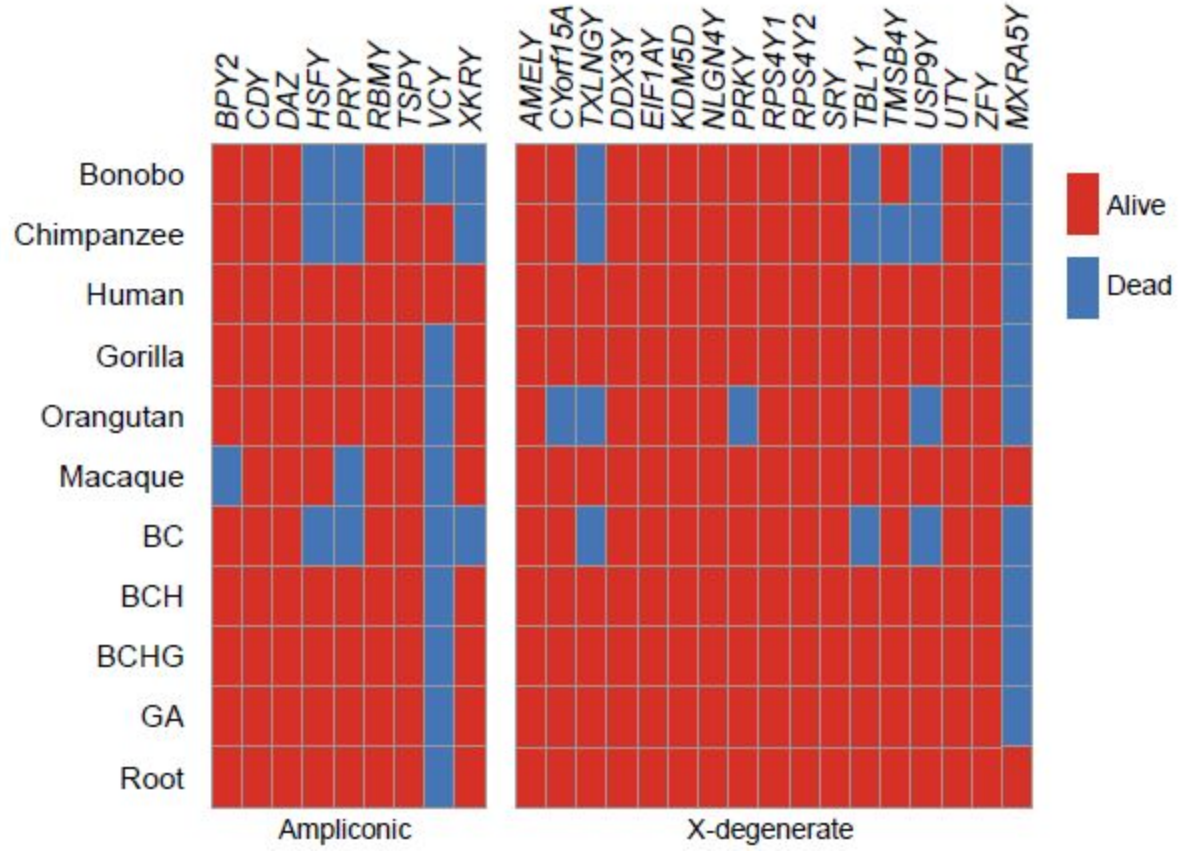

Figure S7. IGV screen shots of peaks of DNase-seq, H3K4me1 and H3K27ac marks on human palindrome P6, and of CREB1 on human palindrome P7.

A. Peaks on both arms of P6 are shown within the blue and grey boxes. **B**. Zoom-in view of peaks on the left arm of palindrome P6. The coverage track represents the depth of coverage and peaks track represents the peaks identified by MACS2 (44). **C**. Zoom-in view of peaks on the right arm of palindrome P6. The coverage track (top) represents the depth of coverage, and the peaks track (bottom) represents the peaks identified by MACS2 (44). **D.** Peaks on both arms of palindrome P7 are shown. The coverage track (top) represents the depth of coverage and the peaks track (bottom) represents the peaks identified by MACS2 (44). See Table S12 for the coordinates of P7.

A

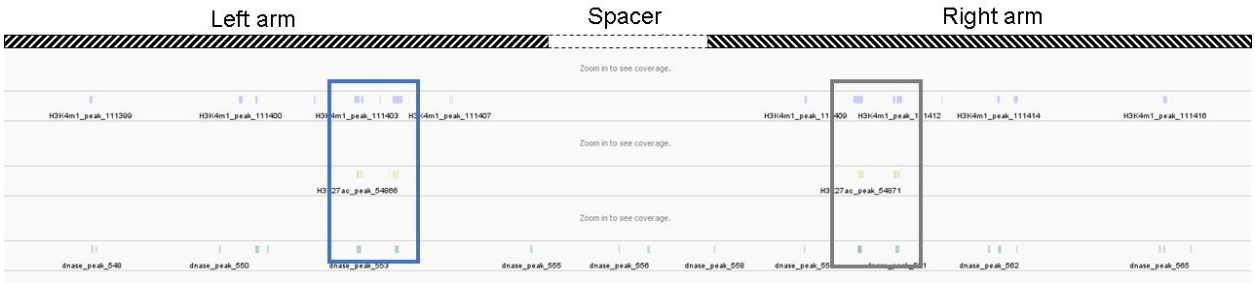

B

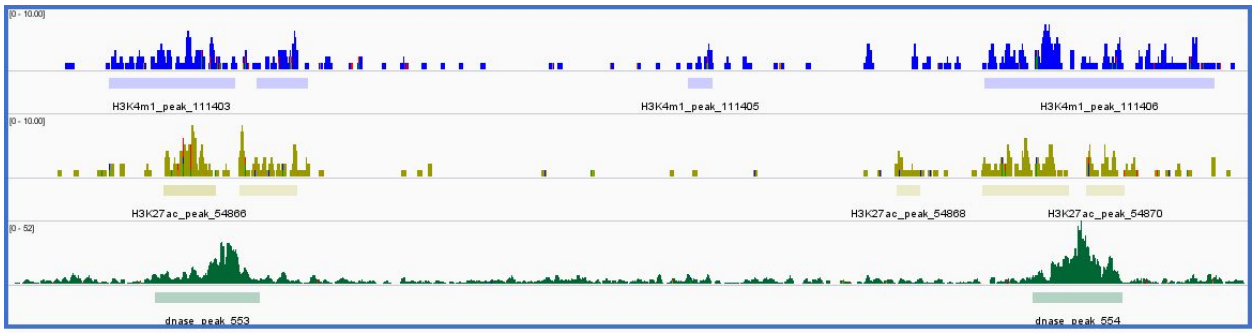

C

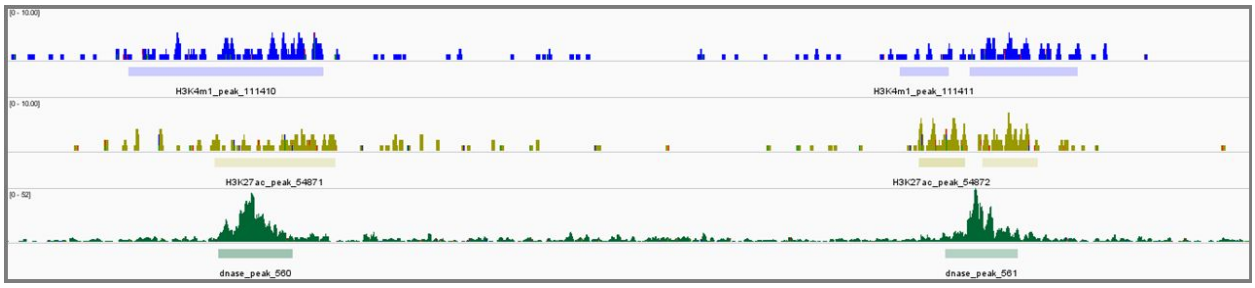

D

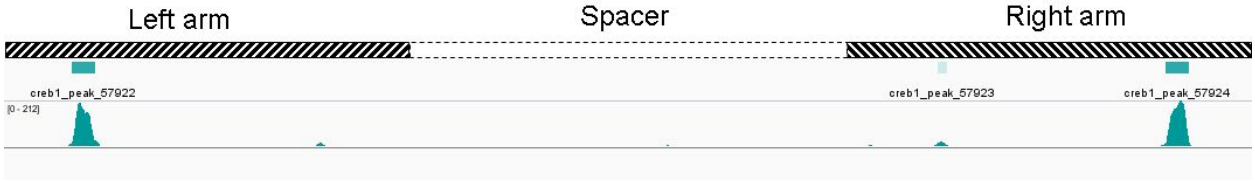

Figure S8. Chromatin interactions on the human Y chromosome.

A. Chromatin contacts split by groups: palindrome-palindrome contacts, palindrome-other (i.e. mixed) and other-other (chromatin interactions in which palindromes are not involved). **B**. The probability of interactions as estimated by (46); the probability is the highest for the palindromic group, in which both reads from a pair fall into human palindromes. The table is based on human iPSC data (47). See also Table S9.

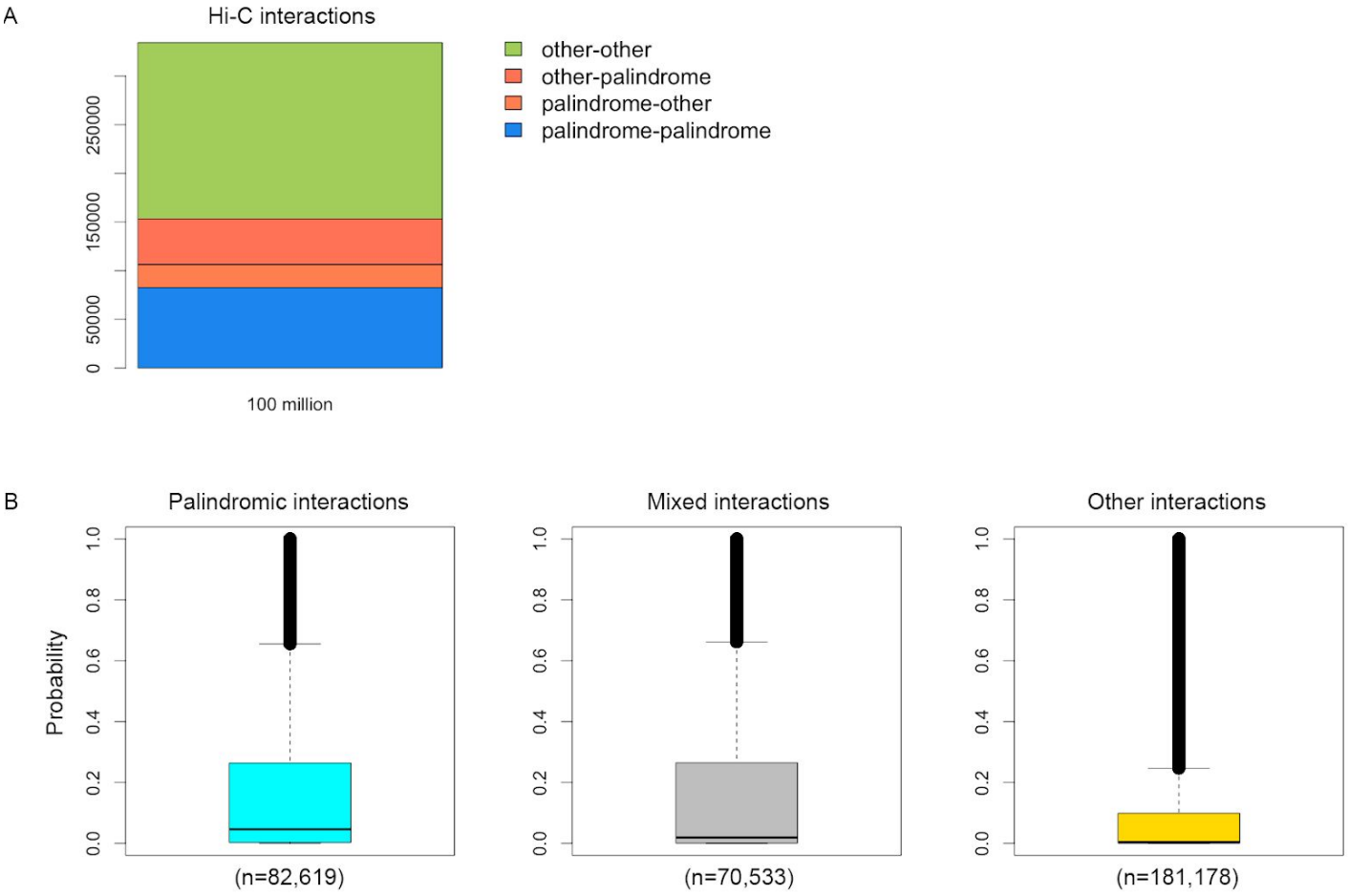

Figure S9. Hi-C contact map generated for Human Umbilical Vein Cells (HUVEC), using the data from (49).

See color coding explained in Fig. 4.

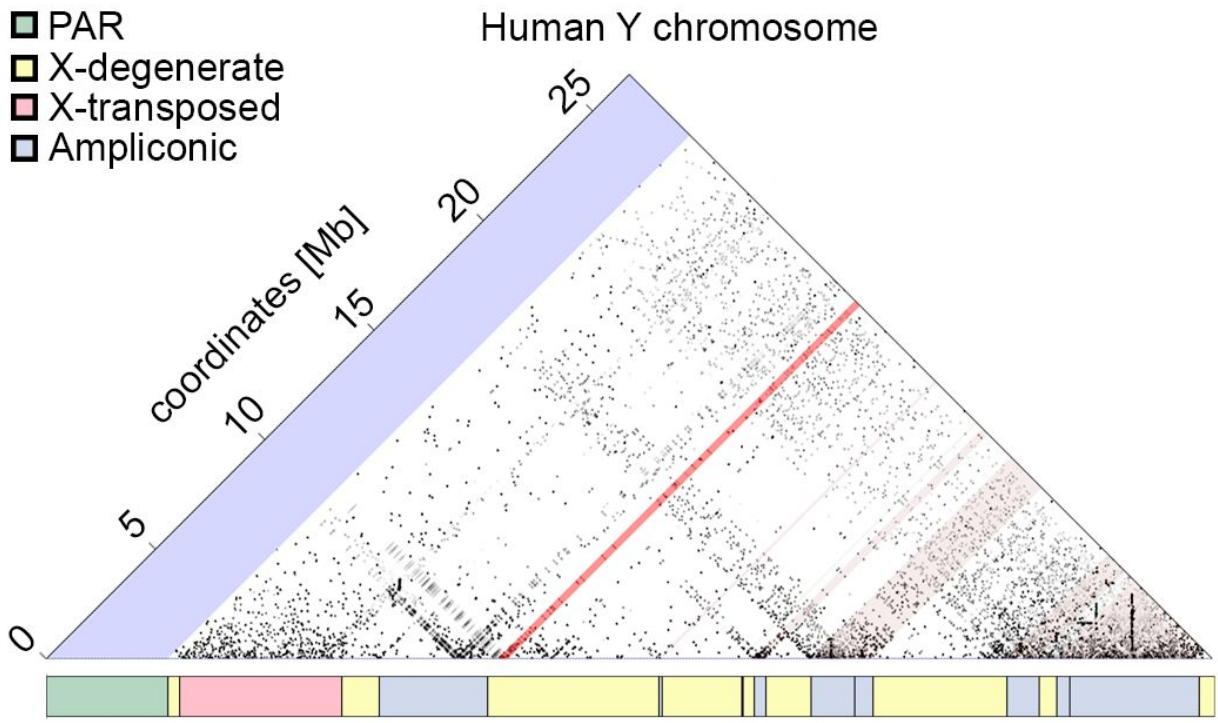

Figure S10. Chromatin contacts on the human and chimpanzee Y chromosomes, as evaluated from iPSCs.

Chromatin interactions for the palindromes P2, P4, and P6 on the human Y. Palindromes similar or smaller in size to the 20 kb bins (i.e. P7 and P8) from the mHi-C pipeline could not be displayed. To resolve ambiguity due to multi-mapping reads, each interaction was assigned a probability based on the fraction of reads supporting it (see Supplemental Methods for details). Palindrome arms are shown as blue arrows and the spacer is shown as white space between them.

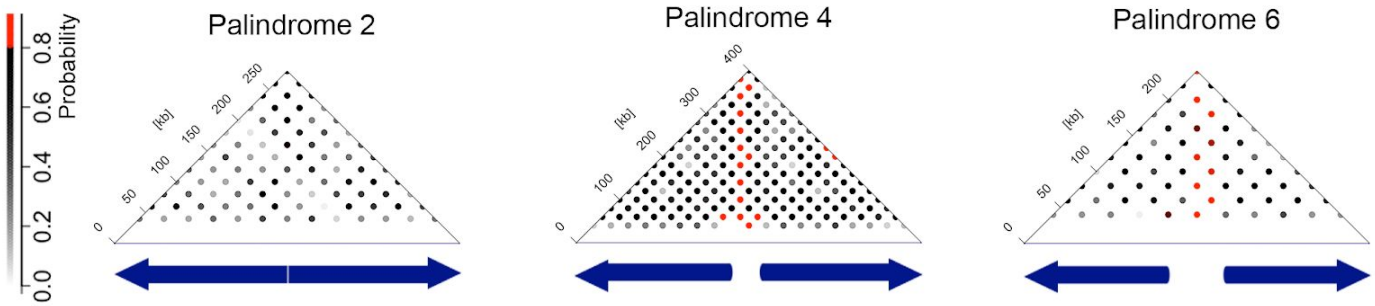

References

1. J. F. Hughes, *et al.*, Chimpanzee and human Y chromosomes are remarkably divergent in structure and gene content. *Nature* **463**, 536–539 (2010).

2. H. Skaletsky, *et al.*, The male-specific region of the human Y chromosome is a mosaic of discrete sequence classes. *Nature* **423**, 825–837 (2003).

3. R. S. Harris, Improved pairwise Alignmnet of genomic DNA (2007).

4. M. Tomaszkiewicz, *et al.*, A time- and cost-effective strategy to sequence mammalian Y Chromosomes: an application to the de novo assembly of gorilla Y. *Genome Res.* **26**, 530–540 (2016).

5. S. Warris, *et al.*, Correcting palindromes in long reads after whole-genome amplification. *BMC Genomics* **19**, 798 (2018).

6. A. H. Wences, M. C. Schatz, Metassembler: merging and optimizing de novo genome assemblies. *Genome Biol.* **16**, 207 (2015).

7. N. I. Weisenfeld, *et al.*, Comprehensive variation discovery in single human genomes. *Nat. Genet.* **46**, 1350–1355 (2014).

8. S. Rangavittal, *et al.*, DiscoverY: a classifier for identifying Y chromosome sequences in male assemblies. *BMC Genomics* **20**, 641 (2019).

9. K. Sahlin, F. Vezzi, B. Nystedt, J. Lundeberg, L. Arvestad, BESST--efficient scaffolding of large fragmented assemblies. *BMC Bioinformatics* **15**, 281 (2014).

10. H. Li, Aligning sequence reads, clone sequences and assembly contigs with BWA-MEM. *arXiv [q-bio.GN]* (2013).

11. N. I. Weisenfeld, V. Kumar, P. Shah, D. M. Church, D. B. Jaffe, Direct determination of diploid genome sequences. *Genome Res.* **27**, 757–767 (2017).

12. M. Boetzer, W. Pirovano, SSPACE-LongRead: scaffolding bacterial draft genomes using long read sequence information. *BMC Bioinformatics* **15**, 211 (2014).

13. A. C. English, *et al.*, Mind the gap: upgrading genomes with Pacific Biosciences RS long-read sequencing technology. *PLoS One* **7**, e47768 (2012).

14. E. Garrison, G. Marth, Haplotype-based variant detection from short-read sequencing. *arXiv [q-bio.GN]* (2012).

15. M. J. Chaisson, G. Tesler, Mapping single molecule sequencing reads using basic local alignment with successive refinement (BLASR): application and theory. *BMC Bioinformatics* **13**, 238 (2012).

16. I. Minkin, P. Medvedev, Scalable multiple whole-genome alignment and locally collinear block construction with SibeliaZ. *bioRxiv*, 548123 (2019).

17. M. Blanchette, *et al.*, Aligning multiple genomic sequences with the threaded blockset aligner. *Genome Res.* **14**, 708–715 (2004).

18. B. Paten, *et al.*, Cactus: Algorithms for genome multiple sequence alignment. *Genome Res.* **21**, 1512–1528 (2011).

19. SMIT, F. A. A., Repeat-Masker Open-3.0. *http://www.repeatmasker.org* (2004) (October 23, 2018).

20. G. Hickey, B. Paten, D. Earl, D. Zerbino, D. Haussler, HAL: a hierarchical format for storing and analyzing multiple genome alignments. *Bioinformatics* **29**, 1341–1342 (2013).

21. D. Earl, *et al.*, Alignathon: a competitive assessment of whole-genome alignment methods. *Genome Res.* **24**, 2077–2089 (2014).

22. P. Moorjani, C. E. G. Amorim, P. F. Arndt, M. Przeworski, Variation in the molecular clock of primates. *Proc. Natl. Acad. Sci. U. S. A.* **113**, 10607–10612 (2016).

23. D. Darriba, G. L. Taboada, R. Doallo, D. Posada, jModelTest 2: more models, new heuristics and parallel computing. *Nat. Methods* **9**, 772 (2012).

24. S. Guindon, O. Gascuel, A simple, fast, and accurate algorithm to estimate large phylogenies by maximum likelihood. *Syst. Biol.* **52**, 696–704 (2003).

25. A. Siepel, D. Haussler, Phylogenetic estimation of context-dependent substitution rates by maximum likelihood. *Mol. Biol. Evol.* **21**, 468–488 (2004).

26. S. Tavaré, Some probabilistic and statistical problems in the analysis of DNA sequences. *Lectures on mathematics in the life sciences* **17**, 57–86 (1986).

27. E. Paradis, J. Claude, K. Strimmer, APE: Analyses of Phylogenetics and Evolution in R language. *Bioinformatics* **20**, 289–290 (2004).

28. M. J. Hubisz, K. S. Pollard, A. Siepel, PHAST and RPHAST: phylogenetic analysis with space/time models. *Briefings in Bioinformatics* **12**, 41–51 (2011).

29. R. Vegesna, *et al.*, Ampliconic genes on the great ape Y chromosomes: Rapid evolution of copy number but conservation of expression levels. *Accepted in GBE* (2020).

30. M. Stanke, S. Waack, Gene prediction with a hidden Markov model and a new intron submodel. *Bioinformatics* **19 Suppl 2**, ii215–25 (2003).

31. S. F. Altschul, W. Gish, W. Miller, E. W. Myers, D. J. Lipman, Basic local alignment search tool. *J. Mol. Biol.* **215**, 403–410 (1990).

32. E. Boutet, *et al.*, UniProtKB/Swiss-Prot, the Manually Annotated Section of the UniProt KnowledgeBase: How to Use the Entry View. *Methods Mol. Biol.* **1374**, 23–54 (2016).

33. W. Iwasaki, T. Takagi, Reconstruction of highly heterogeneous gene-content evolution across the three domains of life. *Bioinformatics* **23**, i230–9 (2007).

34. D. P. Locke, *et al.*, Comparative and demographic analysis of orang-utan genomes. *Nature* **469**, 529–533 (2011).

35. W. J. Kent, *et al.*, The Human Genome Browser at UCSC. *Genome Research* **12**, 996–1006 (2002).

36. J. Krumsiek, R. Arnold, T. Rattei, Gepard: a rapid and sensitive tool for creating dotplots on genome scale. *Bioinformatics* **23**, 1026–1028 (2007).

37. P. J. A. Cock, *et al.*, Biopython: freely available Python tools for computational molecular biology and bioinformatics. *Bioinformatics* **25**, 1422–1423 (2009).

38. W. Miller, *et al.*, 28-Way vertebrate alignment and conservation track in the UCSC Genome Browser. *Genome Research* **17**, 1797–1808 (2007).

39. H. Li, *et al.*, The Sequence Alignment/Map format and SAMtools. *Bioinformatics* **25**, 2078–2079 (2009).

40. F. Ramírez, *et al.*, deepTools2: a next generation web server for deep-sequencing data analysis. *Nucleic Acids Res.* **44**, W160–5 (2016).

41. A. R. Quinlan, I. M. Hall, BEDTools: a flexible suite of utilities for comparing genomic features. *Bioinformatics* **26**, 841–842 (2010).

42. I. Dunham, *et al.*, An integrated encyclopedia of DNA elements in the human genome. *Nature* **489**, 57–74 (2012).

43. C. A. Davis, *et al.*, The Encyclopedia of DNA elements (ENCODE): data portal update. *Nucleic Acids Res.* **46**, D794–D801 (2018).

44. J. M. Gaspar, Improved peak-calling with MACS2. *bioRxiv*, 496521 (2018).

45. J. T. Robinson, *et al.*, Integrative genomics viewer. *Nat. Biotechnol.* **29**, 24–26 (2011).

46. Y. Zheng, F. Ay, S. Keles, Generative modeling of multi-mapping reads with mHi-C advances analysis of Hi-C studies. *eLife* **8** (2019).

47. I. E. Eres, K. Luo, C. J. Hsiao, L. E. Blake, Y. Gilad, Reorganization of 3D genome structure may contribute to gene regulatory evolution in primates. *PLoS Genet.* **15**, e1008278 (2019).

48. P. A. Knight, D. Ruiz, A fast algorithm for matrix balancing. *IMA J. Numer. Anal.* **33**, 1029–1047 (2013).

49. S. S. P. Rao, *et al.*, A 3D map of the human genome at kilobase resolution reveals principles of chromatin looping. *Cell* **159**, 1665–1680 (2014).

50. M. Tomaszkiewicz, P. Medvedev, K. D. Makova, Y and W Chromosome Assemblies: Approaches and Discoveries. *Trends Genet.* **33**, 266–282 (2017).

51. R. Vegesna, M. Tomaszkiewicz, P. Medvedev, K. D. Makova, Dosage regulation, and variation in gene expression and copy number of human Y chromosome ampliconic genes. *PLoS Genet.* **15**, e1008369 (2019).

52. T. Derrien, *et al.*, Fast computation and applications of genome mappability. *PLoS One* **7**, e30377 (2012).

53. A. Zeileis, G. Grothendieck, zoo:S3Infrastructure for Regular and Irregular Time Series. *Journal of Statistical Software* **14** (2005).

54. T. Miyata, H. Hayashida, K. Kuma, K. Mitsuyasu, T. Yasunaga, Male-driven molecular evolution: a model and nucleotide sequence analysis. *Cold Spring Harb. Symp. Quant. Biol.* **52**, 863–867 (1987).

55. K. D. Makova, W.-H. Li, Strong male-driven evolution of DNA sequences in humans and apes. *Nature* **416**, 624–626 (2002).

56. M. A. Wilson Sayres, Genetic Diversity on the Sex Chromosomes. *Genome Biol. Evol.* **10**, 1064–1078 (2018).

57. N. Yu, M. I. Jensen-Seaman, L. Chemnick, O. Ryder, W.-H. Li, Nucleotide Diversity in Gorillas. *Genetics* **166**, 1375–1383 (2004).

58. J.-M. Chen, D. N. Cooper, N. Chuzhanova, C. Férec, G. P. Patrinos, Gene conversion: mechanisms, evolution and human disease. *Nat. Rev. Genet.* **8**, 762–775 (2007).

59. A. J. Jeffreys, C. A. May, Intense and highly localized gene conversion activity in human meiotic crossover hot spots. *Nat. Genet.* **36**, 151–156 (2004).

60. S. A. Sawyer, GENECONV: a computer package for the statistical detection of gene conversion. Distributed by the author, Department of Mathematics, Washington University in St. Louis. *St. Louis* (1999).

61. Z. Yang, PAML: a program package for phylogenetic analysis by maximum likelihood. *Comput. Appl. Biosci.* **13**, 555–556 (1997).

62. M. A. Larkin, *et al.*, Clustal W and Clustal X version 2.0. *Bioinformatics* **23**, 2947–2948 (2007).

63. N. Saitou, M. Nei, The neighbor-joining method: a new method for reconstructing phylogenetic trees. *Mol. Biol. Evol.* **4**, 406–425 (1987).

64. S. Kumar, G. Stecher, K. Tamura, MEGA7: Molecular Evolutionary Genetics Analysis Version 7.0 for Bigger Datasets. *Mol. Biol. Evol.* **33**, 1870–1874 (2016).

65. M. Iwase, Y. Satta, H. Hirai, Y. Hirai, N. Takahata, Frequent gene conversion events between the X and Y homologous chromosomal regions in primates. *BMC Evol. Biol.* **10**, 225 (2010).

66. B. Trombetta, F. Cruciani, P. A. Underhill, D. Sellitto, R. Scozzari, Footprints of X-to-Y gene conversion in recent human evolution. *Mol. Biol. Evol.* **27**, 714–725 (2010).

67. D. Cortez, *et al.*, Origins and functional evolution of Y chromosomes across mammals. *Nature* **508**, 488–493 (2014).

68. X. M. Li, P. H. Yen, L. J. Shapiro, Characterization of a low copy repetitive element S232 involved in the generation of frequent deletions of the distal short arm of the human X chromosome. *Nucleic Acids Res.* **20**, 1117–1122 (1992).

69. M. A. Wilson, K. D. Makova, Evolution and survival on eutherian sex chromosomes. *PLoS Genet.* **5**, e1000568 (2009).

70. B. K. Bhowmick, Y. Satta, N. Takahata, The origin and evolution of human ampliconic gene families and ampliconic structure The origin and evolution of human ampliconic gene families and ampliconic structure. 441–450 (2007).

71. J. F. Hughes, *et al.*, Strict evolutionary conservation followed rapid gene loss on human and rhesus y chromosomes. *Nature* **483**, 82–87 (2012).

72. A. C. E. Darling, B. Mau, F. R. Blattner, N. T. Perna, Mauve: multiple alignment of conserved genomic sequence with rearrangements. *Genome Res.* **14**, 1394–1403 (2004).